John Barnard
Steven Lund
USPAS
June 13-24, 2011
Melville, NY

Mismatched Beams and Beam Halo

Envelope modes of beams in continuous focusing

Envelope modes of bunched beams in continuous focusing

Halos from mismatched beams

CONTINUOUS FOCUSING ENVELOPE MODES

- If $\frac{d}{ds}\gamma\beta = 0$ & $K(s) = k_{p0}^2 = \text{constant}$ & $\epsilon_x = \epsilon_y$

$$\Rightarrow \quad r_x'' + k_{p0}^2 r_x - \frac{2Q}{r_x + r_y} - \frac{\epsilon^2}{r_x^3} = 0 \qquad (s1)$$

$$r_y'' + k_{p0}^2 r_y - \frac{2Q}{r_x + r_y} - \frac{\epsilon^2}{r_y^3} = 0$$

THE EQUILIBRIUM OCCURS WHEN $r_x'' = r_y'' = 0$
& $r_x = r_y = r_b$

- $$\Rightarrow \quad k_{p0}^2 r_b - \frac{Q}{r_b} - \frac{\epsilon^2}{r_b^3} = 0$$

THIS IS EASILY SOLVED FOR r_b:

$$r_b = \frac{Q^{1/2}}{k_{p0}} \left[\frac{1}{2} + \frac{1}{2}\sqrt{1 + 4k_{p0}^2\epsilon^2/Q^2}\right]^{1/2} \rightarrow \begin{cases} \frac{Q^{1/2}}{k_{p0}}; & \frac{2k_{p0}\epsilon}{Q} \ll 1 \\ \frac{\epsilon^{1/2}}{k_{p0}^{1/2}}; & \frac{2k_{p0}\epsilon}{Q} \gg 1 \end{cases}$$

Let $\quad r_x = r_b + \xi(s)$

$\quad r_y = r_b + \eta(s)$

LINEARIZING (S1)

$$(S1) \Rightarrow 0 = \xi'' + k_{p0}^2 (r_b + \xi) - \frac{2Q}{2r_b}\left(1 - \frac{\xi}{2r_b} - \frac{\eta}{2r_b}\right) - \frac{\epsilon^2}{r_b^3}\left(1 - \frac{3\xi}{r_b}\right)$$

$$\& \quad 0 = \eta'' + k_{p0}^2 (r_b + \eta) - \frac{2Q}{2r_b}\left(1 - \frac{\xi}{2r_b} - \frac{\eta}{2r_b}\right) - \frac{\epsilon^2}{r_b^3}\left(1 - \frac{3\eta}{r_b}\right)$$

SUBTRACTING THE EQUILIBRIUM:

$$\xi'' + \left(k_{p0}^2 + \frac{Q}{2r_b^2} + \frac{3\epsilon^2}{r_b^4}\right)\xi + \frac{Q}{2r_b^2}\eta = 0$$

$$\eta'' + \left(k_{p0}^2 + \frac{Q}{2r_b^2} + \frac{3\epsilon^2}{r_b^4}\right)\eta + \frac{Q}{2r_b^2}\xi = 0$$

USING $\quad k_p^2 = k_{p0}^2 - \frac{Q}{r_b^2} = \frac{\epsilon^2}{r_b^4}$

$$\Rightarrow \quad \xi'' + \left(\tfrac{3}{2}k_{p0}^2 + \tfrac{5}{2}k_p^2\right)\xi + \left(\tfrac{1}{2}k_{p0}^2 - \tfrac{1}{2}k_p^2\right)\eta = 0 \qquad (A)$$

$$\eta'' + \left(\tfrac{3}{2}k_{p0}^2 + \tfrac{5}{2}k_p^2\right)\eta + \left(\tfrac{1}{2}k_{p0}^2 - \tfrac{1}{2}k_p^2\right)\xi = 0 \qquad (B)$$

LET $\varphi_1 = \xi - \eta$ SUBTRACTING (B) FROM (A):

$$\varphi_1'' + k_1^2 \varphi_1 = 0$$

Where $k_1^2 = \left(\tfrac{3}{2}k_{p0}^2 + \tfrac{5}{2}k_p^2 - \tfrac{1}{2}k_{p0}^2 + \tfrac{1}{2}k_p^2\right) = k_{p0}^2 + 3k_p^2$

LET $\varphi_2 = \xi + \eta$ ADDING (A) & (B):

$$\varphi_2'' + k_2^2 \varphi_2 = 0$$

where $k_2^2 = \left(\tfrac{3}{2}k_{p0}^2 + \tfrac{5}{2}k_p^2 + \tfrac{1}{2}k_{p0}^2 - \tfrac{1}{2}k_p^2\right) = 2k_{p0}^2 + 2k_p^2$

Letting $\xi = \xi_0 e^{ik_1 s}$ $\eta = \eta_0 e^{ik_1 s}$ where $k_1^2 = k_{p0}^2 + 3k_p^2$

(A) $\Rightarrow$

$$-(k_{p0}^2 + 3k_p^2)\xi_0 + (\tfrac{3}{2}k_{p0}^2 + \tfrac{5}{2}k_p^2)\xi_0 + (\tfrac{1}{2}k_{p0}^2 - \tfrac{1}{2}k_p^2)\eta_0 = 0$$

$$\Rightarrow \quad \tfrac{1}{2}(k_{p0}^2 - k_p^2)[\xi_0 + \eta_0] = 0 \qquad (A')$$

(B) $$-(k_{p0}^2 + 3k_p^2)\eta_0 + (\tfrac{3}{2}k_{p0}^2 + \tfrac{5}{2}k_p^2)\eta_0 + (\tfrac{1}{2}k_{p0}^2 - \tfrac{1}{2}k_p^2)\xi_0 = 0$$

$$\Rightarrow \tfrac{1}{2}(k_{p0}^2 - k_p^2)[\xi_0 + \eta_0] = 0 \qquad (B')$$

Similarly for $\xi = \xi_0 e^{ik_2 s}$ and $\eta = \eta_0 e^{ik_2 s}$

(A) $\Rightarrow$

$$-(2k_{p0}^2 + 2k_p^2)\xi_0 + (\tfrac{3}{2}k_{p0}^2 + \tfrac{5}{2}k_p^2)\xi_0 + (\tfrac{1}{2}k_{p0}^2 - \tfrac{1}{2}k_p^2)\eta_0 = 0$$

$$\Rightarrow \tfrac{1}{2}(k_{p0}^2 - k_p^2)[-\xi_0 + \eta_0] = 0 \qquad (A'')$$

(B) $\Rightarrow$

$$-(2k_{p0}^2 + 2k_p^2)\eta_0 + (\tfrac{3}{2}k_{p0}^2 + \tfrac{5}{2}k_p^2)\eta_0 + (\tfrac{1}{2}k_{p0}^2 - \tfrac{1}{2}k_p^2)\xi_0 = 0$$

$$\tfrac{1}{2}(k_{p0}^2 - k_{p0}^2)[-\eta_0 + \xi_0] = 0 \qquad (B'')$$

THE SOLUTIONS ARE:

$$y_1 \sim e^{ik_1 s} \Rightarrow \xi \& \eta \sim e^{ik_1 s}$$

EQUATIONS (A') & (B') CAN BE WRITTEN

$$\begin{pmatrix} 1 & 1 \\ 1 & 1 \end{pmatrix}\begin{pmatrix} \xi \\ \eta \end{pmatrix} = 0 \Rightarrow \xi = -\eta \Rightarrow \text{"QUADRUPOLE MODE"}$$

FOR $y_2 \sim e^{ik_2 s}$ THE MATRIX EQUATIONS (A") & (B") BECOMES:

$$\begin{pmatrix} -1 & 1 \\ 1 & -1 \end{pmatrix}\begin{pmatrix} \xi \\ \eta \end{pmatrix} = 0 \Rightarrow \xi = \eta \Rightarrow \text{"BREATHING MODE"}$$

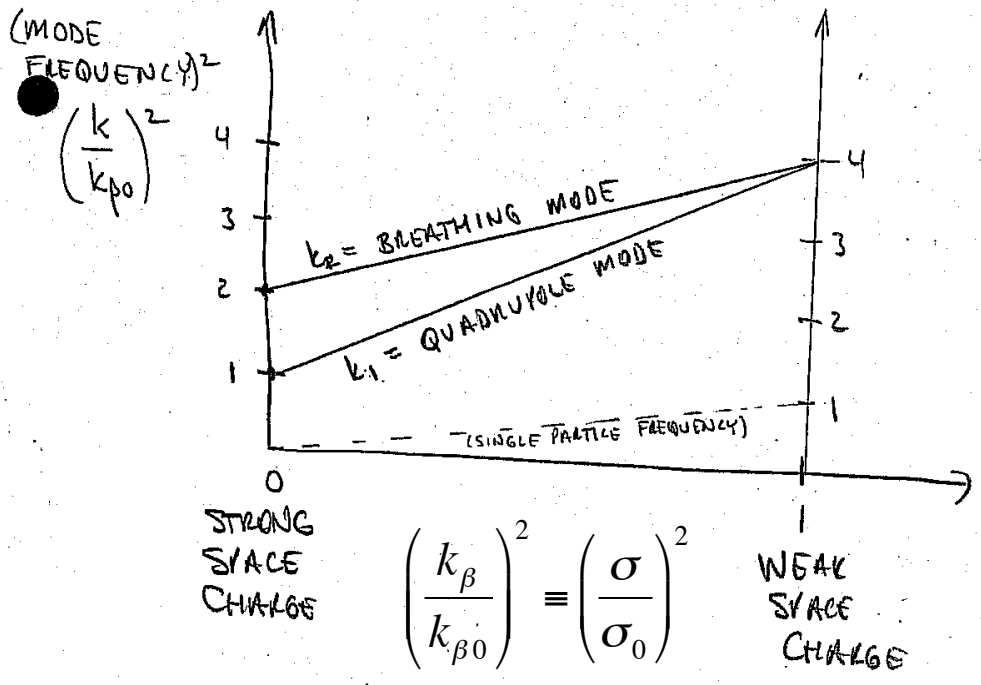

$$k_1^2 = k_{p0}^2 + 3k_p^2 \qquad k_2^2 = 2k_{p0}^2 + 2k_p^2 \leftarrow \text{MODE FREQUENCY}$$

$$k_p^2 = k_{p0}^2 - \frac{Q}{r_b^2} \leftarrow \text{SINGLE PARTICLE FREQUENCY}$$

Continuous focusing: breathing mode and quadrupole mode

Breathing mode:

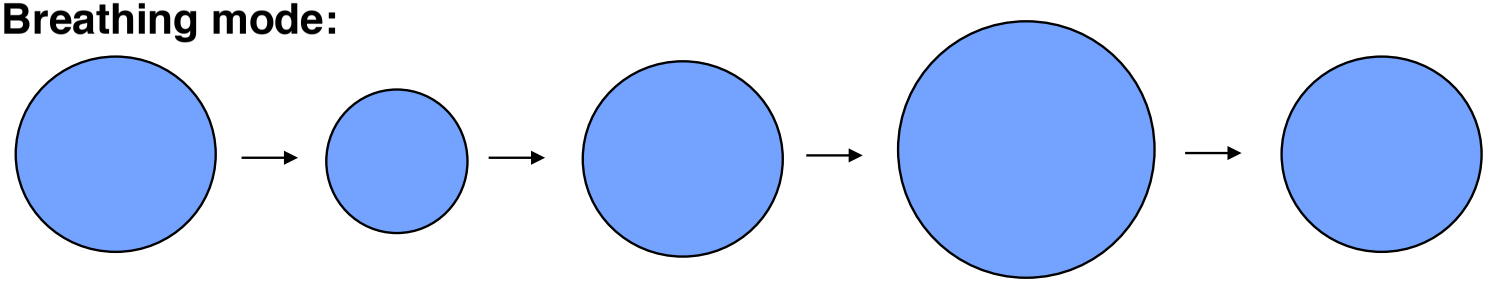

Quadrupole mode:

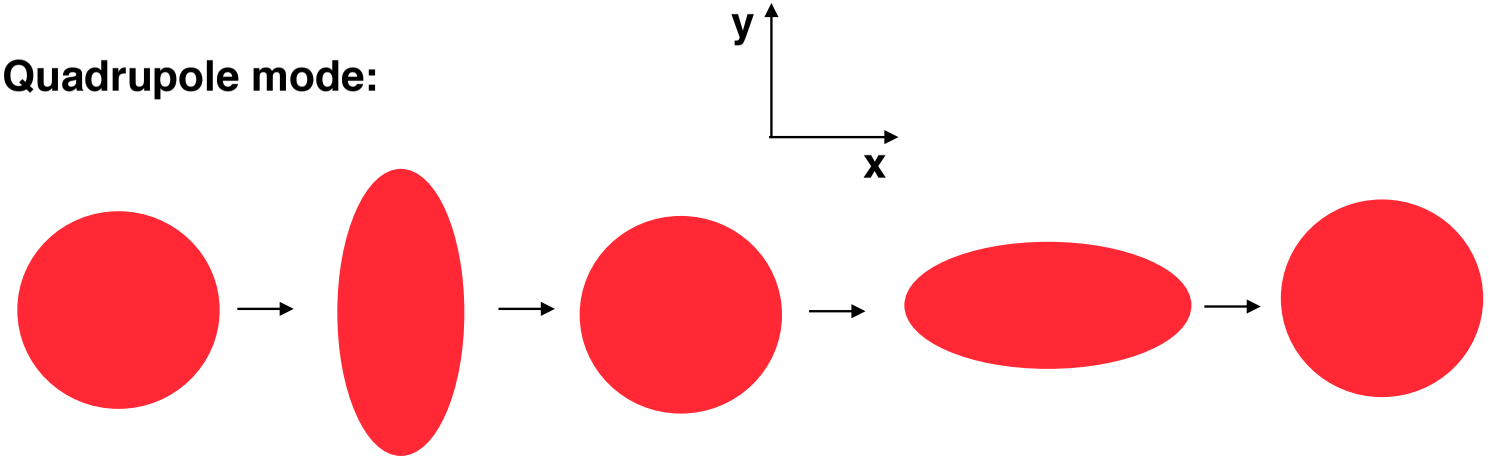

Note that in the quadrupole mode the beam area is nearly constant, whereas in the breathing mode, density increases increasing restoring force; hence breathing mode has the higher frequency of the two modes.

JOHN BALLARD
& STEVEN LUND
USPAS
JANUARY 2004

(6)

II ENVELOPE MODES OF BUNCHED BEAMS IN CONTINUOUS FOCUSING CHANNELS

Total field seen by particle is sum of rf and spacecharge

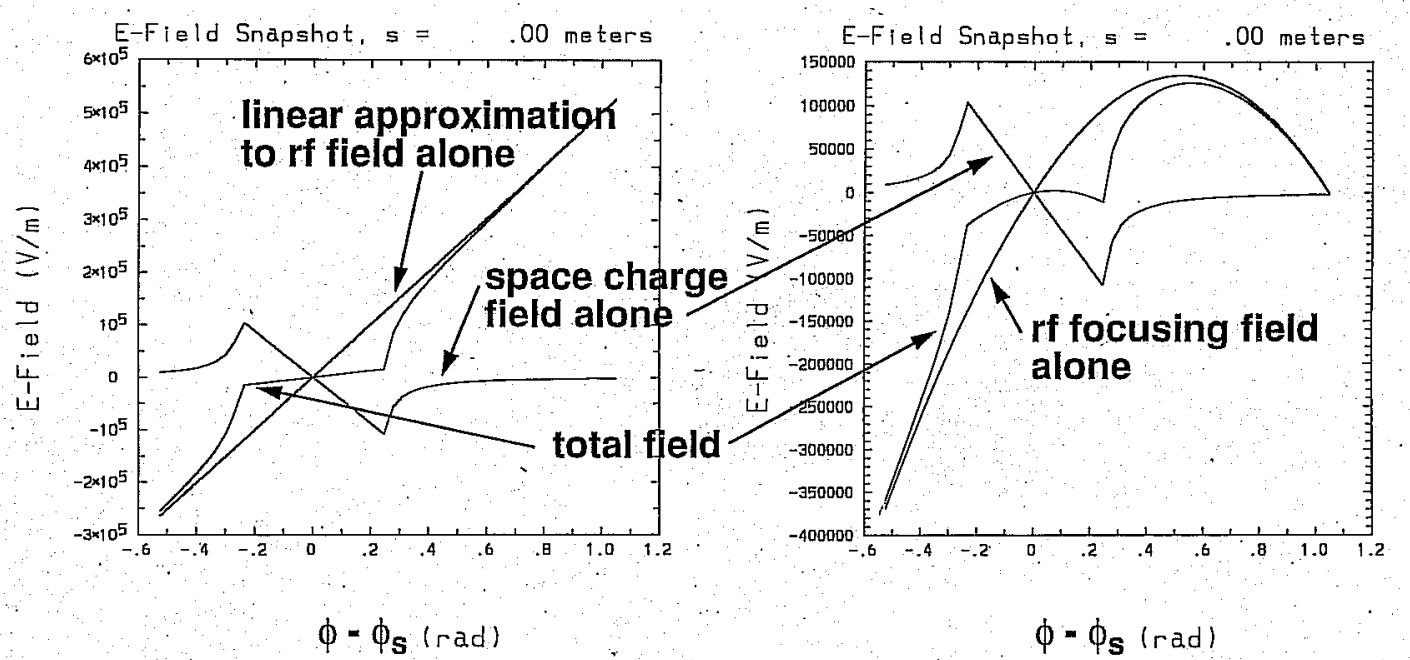

here $\phi - \phi_s = - (2\pi/\beta_s\lambda)\,\Delta z$, where $\beta_s c$ is the longitudinal velocity of the synchronous particle and $\lambda = c/\nu$ is the rf vacuum wavelength

SPACE-CHARGE FIELD OF BUNCHED BEAMS

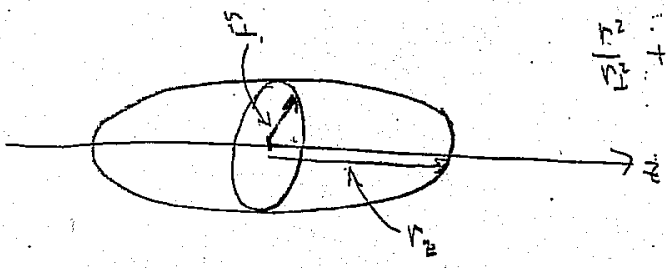

$\frac{r^2}{r_\perp^2} + \frac{z^2}{r_z^2} = 1$ ← BOUNDARY OF ELLIPSOID

THE POTENTIAL OF A UNIFORM DENSITY BUNCH IN FREE SPACE (A MACLAURIN SPHEROID) IS GIVEN BY:

Conf Landau & Lifshitz, Classical Theory of Fields, (p 247)

$$\psi = \frac{\rho}{4\varepsilon_0}\left(\alpha_\perp r^2 + \alpha_\parallel z^2 - \delta\right)$$

where $\alpha_\perp = r_\perp^2 r_z \int_0^\infty \frac{ds}{(r_\perp^2+s)\Delta}$

$\alpha_\parallel = r_\perp^2 r_z \int_0^\infty \frac{ds}{(r_z^2+s)\Delta}$

$\delta = r_\perp^2 r_z \int_0^\infty \frac{ds}{\Delta}$

where $\Delta^2 = (r_\perp^2+s)^2(r_z^2+s)$

FOR NON-RELATIVISTIC BEAM:

$$E_z = -\frac{\partial\phi}{\partial z} = f\frac{\rho}{\varepsilon_0} z$$

$$E_r = -\frac{\partial\phi}{\partial r} = \frac{(1-f)}{2}\frac{\rho}{\varepsilon_0} r$$

$$f = f(\alpha) = \begin{cases} \frac{\alpha^2}{1-\alpha^2}\left[\frac{1}{\sqrt{1-\alpha^2}}\tanh^{-1}\sqrt{1-\alpha^2} - 1\right] & \alpha < 1 \\ \frac{1}{3} & \alpha = 1 \\ \frac{\alpha^2}{\alpha^2-1}\left[1 - \frac{1}{\sqrt{\alpha^2-1}}\tan^{-1}\sqrt{\alpha^2-1}\right] & \alpha > 1 \end{cases} \qquad \alpha \equiv \frac{r_\perp}{r_z}$$

FOR RELATIVISTIC BEAM

(cf. Lund & Bazlard 1997 PAC97 Conf. Proceedings, Vancouver)

$$\frac{d^2 \underline{x}_\perp}{ds^2} = \frac{F_\perp}{\gamma_s \beta_s^2 mc^2}$$

$$F_{\perp s} = \frac{-q}{\gamma_s^2} \frac{\partial \phi}{\partial \underline{x}_\perp} = \frac{q\rho}{2\gamma_s^2 \epsilon_0} [1 - f(\alpha)] \underline{x}_\perp$$

$$\frac{d^2 \Delta z}{ds^2} = \frac{F_z}{\gamma_s^3 \beta_s^2 mc^2}$$

$$F_{zs} = \frac{-q}{\gamma_s^2} \frac{\partial \phi}{\partial z} = \frac{q\rho}{\epsilon_0} f(\alpha) \Delta z$$

$$\alpha = \frac{r_\perp}{\gamma r_z} \qquad \left[\alpha = \frac{r_\perp}{(r_z \text{ in comoving frame})} \right]$$

COMBINING FOCUSING & SELF FIELDS

$$\frac{d^2}{ds^2} \Delta z = -k_{z0}^2 \Delta z + \frac{q\rho f(\alpha)}{\gamma_s^3 \beta_s^2 mc^2 \epsilon_0} \Delta z \qquad \text{(LINEAR rf)}$$

$$\frac{d^2}{ds^2} \underline{x}_\perp = -k_{\beta 0}^2 \underline{x}_\perp + \frac{q\rho [1 - f(\alpha)]}{2\gamma_s^3 \beta_s^2 mc^2 \epsilon_0} \underline{x}_\perp$$

$$\rho = \frac{3I\lambda_{rf}}{4\pi r_\perp^2 r_z c} \qquad \text{where } \lambda_{rf} = \frac{2\pi c}{\omega}$$

Envelope Equations for an Unaccelerated Ellipsoidal Beam Bunch with Uniform Space-Charge

$$\frac{d^2 r_\perp}{ds^2} + k_{\beta 0}^2 r_\perp - \frac{K_{3D}[1 - f(\alpha)]}{2 r_\perp r_z} - \frac{\epsilon_x^2}{r_\perp^3} = 0$$

$$\frac{d^2 r_z}{ds^2} + f_{nl}(\zeta)\, k_{s0}^2 r_z - \frac{K_{3D} f(\alpha)}{r_\perp^2} - \frac{\epsilon_z^2}{r_z^3} = 0$$

$\alpha = \frac{r_\perp}{\gamma r_z}$

$f_{nl}(\zeta) = (15/\zeta^5)[(3 - \zeta^2)\sin\zeta - 3\zeta\cos\zeta]$ Let $\zeta = (2\pi/\beta_s\lambda) r_z$

$k_{\beta 0}^2$	Undepressed Transverse Betatron Wavenumber-Squared
k_{s0}^2	Undepressed Longitudinal Synchrotron Wavenumber-Squared
$K_{3D} = 3qI\lambda/4\pi\epsilon_0\gamma_s^3\beta_s^3 mc^3$	3D Space-Charge Parameter (dimension of length)
$\epsilon_x^2 = 25[\langle x^2\rangle\langle x'^2\rangle - \langle xx'\rangle^2]$	3D Bunched Beam Transverse Emittance-Squared
$\epsilon_z^2 = 25[\langle \Delta z^2\rangle\langle \Delta z'^2\rangle - \langle \Delta z \Delta z'\rangle^2]$	3D Bunched Beam Longitudinal Emittance-Squared
f_{nl}	Accounts for Nonlinear rf Focusing, $f_{nl}(\zeta) \to 1$ when $\zeta \to 0$

- Envelope equations couple the transverse and longitudinal single-particle motion
- Bunch acceleration results in additional terms
- Linear rf envelope equations presented in Wangler, "Intro. to Linear Accelerators"

Envelope Equations will be used to:

- Calculate equilibrium values of the envelope widths r_z and $r_\perp$
- Calculate properties of mismatch eigenmodes
  - Mode wavenumber
  - Relative amplitude of transverse and longitudinal mismatch

$\lambda_{rf} \equiv \frac{2\pi c}{\omega}$ = rf vacuum wavelength

$I \equiv \frac{qN\epsilon}{\lambda_{rf}}$ = average current

$K_{3D} = \frac{3}{2} Q \lambda_{rf}$

Perturbed Envelope Equations
Yield Linear Eigenmode for a Mismatched Ellipsoidal Beam Bunch

Assume small-amplitude perturbations ($|\delta r_\perp|/r_{\perp 0} \ll 1$ and $|\delta r_z|/r_{z0} \ll 1$):

$$\boxed{\begin{aligned} r_\perp &= r_{\perp 0} + \delta r_\perp \exp(iks) \\ r_z &= r_{z0} + \delta r_z \exp(iks) \end{aligned}}$$

See Barnard & Lund
Lund & Barnard
PAC 97 Vancouver
Conf. Proceedings

To obtain coupled linear mode equations:

$$\boxed{\begin{pmatrix} -k^2 + K_{11} & K_{12} \\ K_{21} & -k^2 + K_{22} \end{pmatrix} \begin{pmatrix} \delta r_\perp / r_{\perp 0} \\ \delta r_z / r_{z0} \end{pmatrix} = 0}$$

$$K_{11} = 4k_\beta^2 - \frac{K_{3D}}{r_{\perp 0}^2 r_{z0}} \left[1 - f(\alpha) - \frac{\alpha}{2} \frac{df(\alpha)}{d\alpha} \right]_{r_\perp = r_{\perp 0}, r_z = r_{z0}}$$

$$K_{22} = 4k_{s0}^2 \left[f_{nl}(\zeta) + \frac{\zeta}{4} \frac{df_{nl}(\zeta)}{d\zeta} \right]_{r_\perp = r_{\perp 0}, r_z = r_{z0}} - \frac{3K_{3D}}{r_{\perp 0}^2 r_{z0}} \left[f(\alpha) - \frac{\alpha}{3} \frac{df(\alpha)}{d\alpha} \right]_{r_\perp = r_{\perp 0}, r_z = r_{z0}}$$

$$K_{12} = \frac{K_{3D}}{2r_{\perp 0}^2 r_{z0}} \left[1 - f(\alpha) - \alpha \frac{df(\alpha)}{d\alpha} \right]_{r_\perp = r_{\perp 0}, r_z = r_{z0}}$$

$$K_{21} = \frac{K_{3D}}{r_{\perp 0}^2 r_{z0}} \left[2f(\alpha) - \alpha \frac{df(\alpha)}{d\alpha} \right]_{r_\perp = r_{\perp 0}, r_z = r_{z0}}$$

Solution of the quartic dispersion relation characterizes the envelope mismatch modes

Spatial Frequencies:

High Frequency Mode : $$k^2 = k_H^2 = \frac{1}{2}(K_{11} + K_{22}) + \frac{1}{2}\sqrt{(K_{11} - K_{22})^2 + 4K_{12}K_{21}}$$

Low Frequency Mode : $$k^2 = k_L^2 = \frac{1}{2}(K_{11} + K_{22}) - \frac{1}{2}\sqrt{(K_{11} - K_{22})^2 + 4K_{12}K_{21}}$$

Relative Amplitude of Transverse and Longitudinal Oscillations:

$$\frac{\delta r_\perp / r_{\perp 0}}{\delta r_z / r_{z0}} = \frac{K_{12}}{k^2 - K_{11}}$$

Barnard 21

Envelope equations yield equilibrium beam parameters and eigenfrequencies and modes of mismatched beam

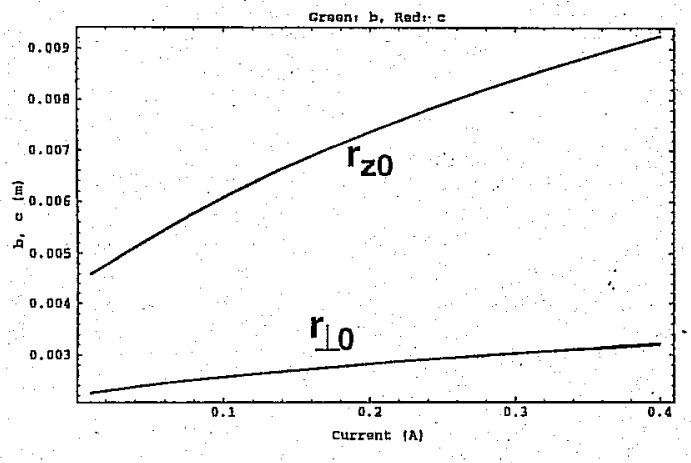

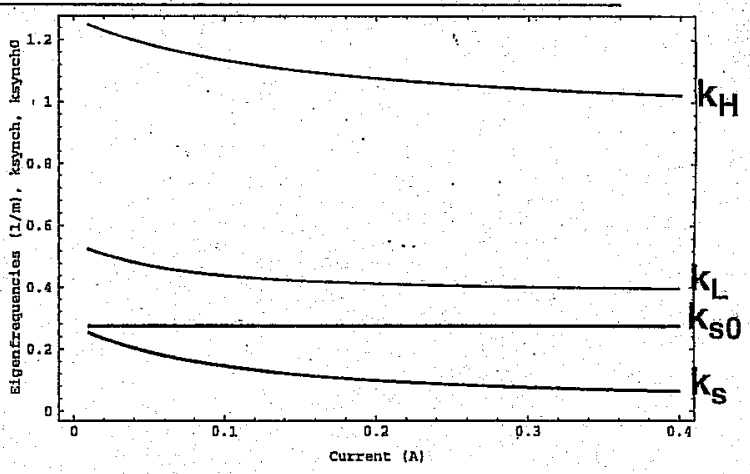

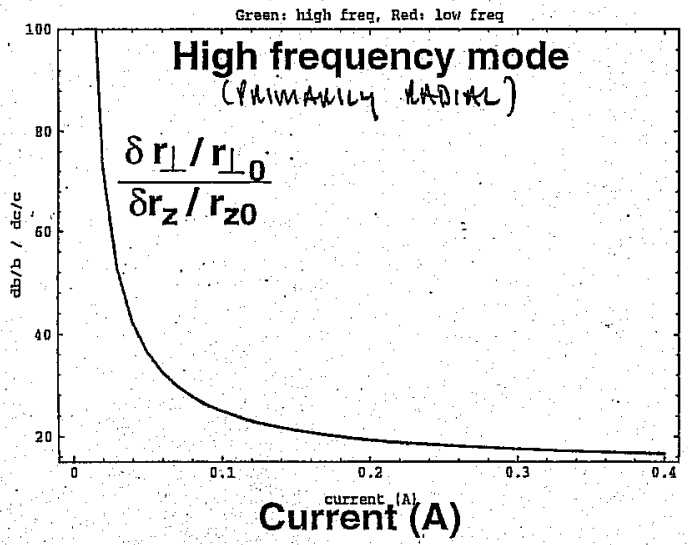

← INCREASING σ/σ_0

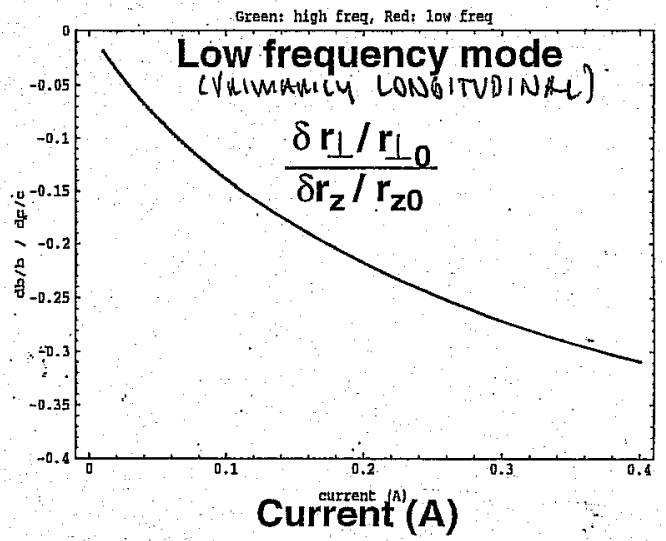

Bunched beams with continuous focusing: low frequency and high frequency modes

High frequency mode (primarily transverse):

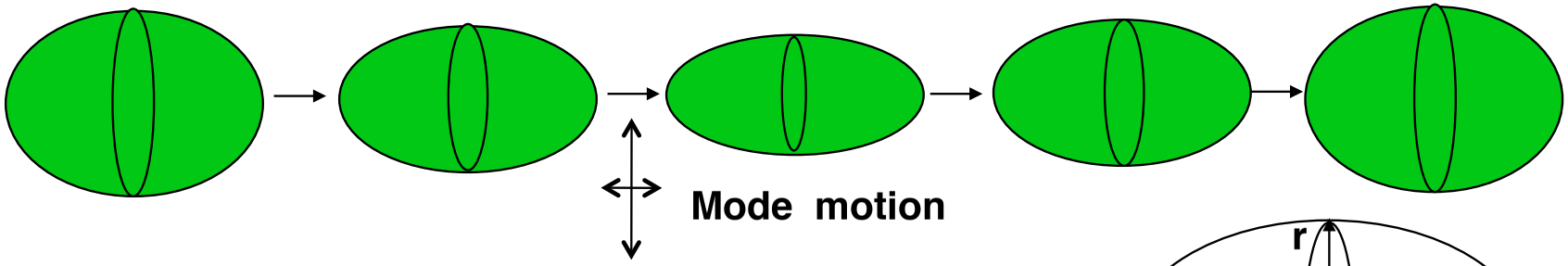

(A second high frequency mode (primarily transverse) corresponds to the quadrupole mode of unbunched beam).

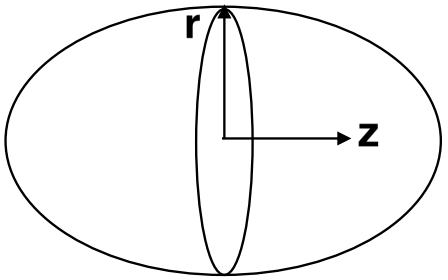

Low frequency mode (primarily longitudinal):

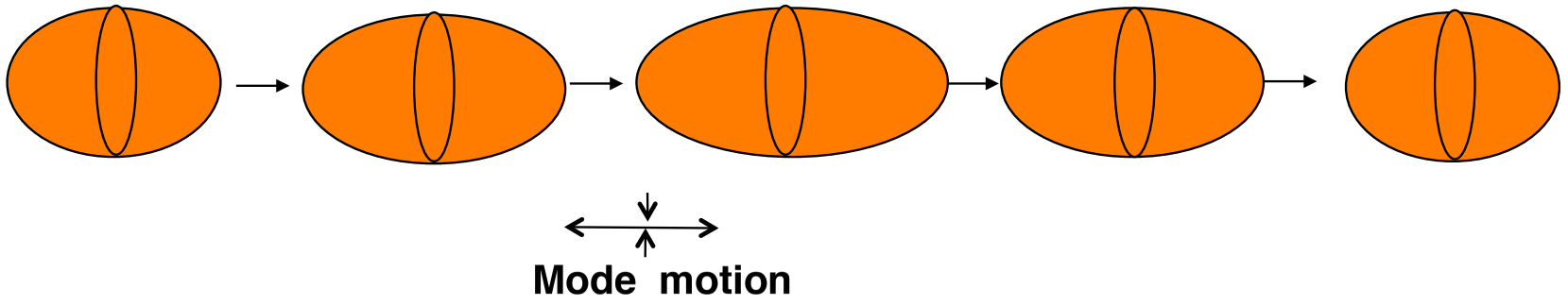

JOHN BARNARD
& STEVEN LUNO
USPAS JANUARY 2004

III HALOS

1. WHAT IS HALO? WHY DO WE CARE?

2. QUALITATIVE PICTURE OF HALO FORMATION:
   MISMATCHES RESONANTLY DRIVE PARTICLES TO LARGE AMPLITUDE

3. CORE/PARTICLE MODELS

4. AMPLITUDE/PHASE ANALYSIS

FULLY SELF-CONSISTENT PIC CODE RESULTS

FROM "BEAM LOSS & BEAM HALO STUDIES" ROBERT RYNE, 1995

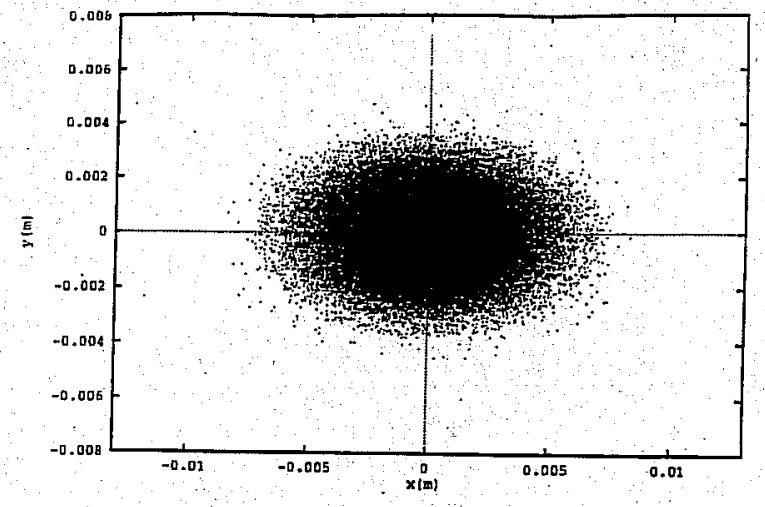

MATCHED BEAM

Figure 5: Beam halo after 22 focusing periods in a FODO channel. The initial distribution is an *rms* matched Gaussian beam. ($\sigma_0 = 70\,\text{deg}$, $\sigma = 35\,\text{deg}$)

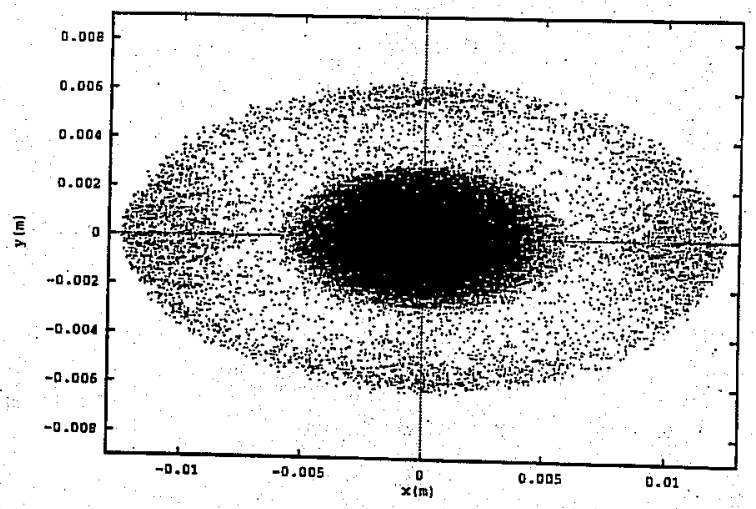

MISMATCHED BEAM

Figure 6: Beam halo after 22 focusing periods in a FODO channel. The initial distribution is an *rms* mismatched Gaussian beam. ($\sigma_0 = 70\,\text{deg}$, $\sigma = 35\,\text{deg}$)

WHY DO WE CARE?

1). BEAM LOSS OF HIGH ENERGY PARTICLES
⇒ ACCELERATOR ACTIVATION

EXAMPLE: FOR THE 1 GeV, 100 mA ACCELERATOR PRODUCTION OF TRITIUM (APT) PARAMETERS
1 nA/m OF BEAM LOSS ALLOWED FOR "HANDS ON" MAINTENANCE (FOR $E \gtrsim 1$ GeV)
($\frac{1\,nA}{m} m \times 1000\,m \Rightarrow 10^{-6}$ A loss allowed).

$\Rightarrow \frac{10^{-6}\,A}{0.1\,A} \Leftrightarrow 10^{-5}$ fractional beam loss allowed !!

2). BEAM LOSS ON WALLS
⇒ ELECTRON / GAS EMISSION FROM WALLS

FOR LONG PULSE OR DC MACHINES, OR STORAGE RINGS, WHERE ELECTRONS CAN BE DRAWN INTO BEAM AND ACCUMULATION ⇒ INSTABILITIES AND NON-LINEAR FIELDS COULD DESTROY BEAM EMITTANCE OR EVEN DISRUPT BEAM.

3). INCREASE IN EMITTANCE

MAY REDUCE FOCUSABILITY FOR APPLICATIONS REQUIRING A SMALL BEAM SPOT.

WHAT IS THE BASIC PHYSICS?

RECALL DISPERSION RELATION FOR ENVELOPE MODES:

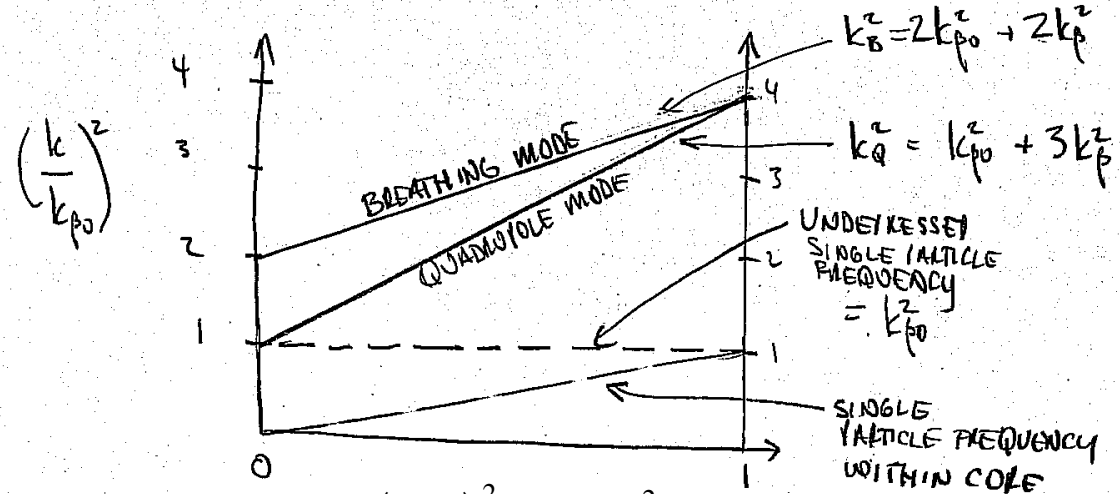

STRONG SPACE CHARGE $\left(\frac{k_\beta}{k_{\beta 0}}\right)^2 \equiv \left(\frac{\sigma}{\sigma_0}\right)^2$ WEAK SPACE CHARGE

CONSIDER DIAGRAM FOR $\frac{k_B}{2}$ AND $\frac{k_Q}{2}$:

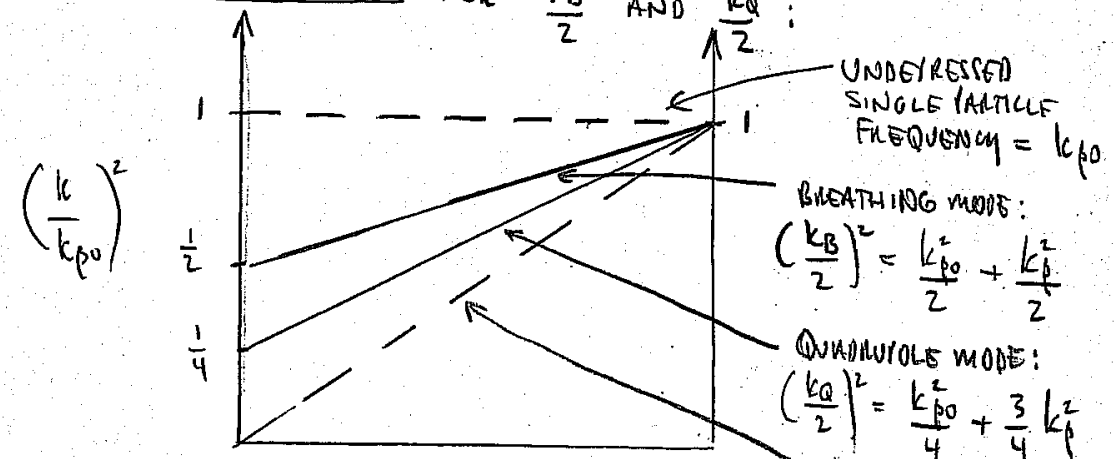

$$\left(\frac{k_\beta}{k_{\beta 0}}\right)^2 \equiv \left(\frac{\sigma}{\sigma_0}\right)^2$$

PARTICLES IN ORBITS FAR FROM CORE OSCILLATE AT FREQUENCY k_{f0}, WHEREAS THOSE WITHIN CORE OSCILLATE AT FREQUENCY k_p.

AT INTERMEDIATE RADII, PARTICLE FREQUENCY = ENVELOPE FREQUENCY /2

$\Rightarrow$ POSSIBILITY OF RESONANCE

$\Rightarrow$ MISMATCHES (EXCITATION OF ENVELOPE MODES) TOGETHER WITH COMMENSURATE PARTICLE FREQUENCY AND ENVELOPE HALF-FREQUENCY ARE THE SOURCE OF HALO.

SUGGESTS USING A CORE/TEST PARTICLE MODE TO EXPLORE THESE EFFECTS (O'CONNELL, WANGLER, JAMESON, RYNE, ...)

ASSUME KV ENVELOPE, OSCILLATING AT A MODE FREQUENCY.

USE KNOWN ANALYTIC FORMULAS INTERIOR AND EXTERIOR TO BEAM.

FOR EXAMPLE, FOR CIRCULAR BEAM

$$x'' = \begin{cases} -\left[k_{p0}^2 - \frac{Q}{r_b^2}\right] x & \text{for } r < r_b \\ -\left[k_{p0}^2 - \frac{Q}{r^2}\right] x & \text{for } r > r_b \end{cases}$$

Similarly for y.

$$r_b = r_{b0} + \delta r_b \cos(k_B s + \phi)$$

k_B ← BREATHING MODE

DISTRIBUTE TEST PARTICLES IN PHASE SPACE AND FOLLOW EVOLUTION OF ORBITS. ALLOWS PHYSICS STUDIES, WHICH CAN BE FOLLOWED UP WITH SELF-CONSISTENT PIC RUNS.

NOTE THAT THE SAME TYPE OF RESONANCES OCCUR LONGITUDINALLY, IN BUNCHED BEAMS.

BETATRON FREQUENCY → SYNCHROTRON FREQUENCY

$k_{\beta 0} \rightarrow k_{s0}$

$k_\beta \rightarrow k_s$ (DEPRESSED) SYNCHROTRON FREQUENCY)

BREATHING MODE $k_B \rightarrow k_L$ LOW FREQUENCY MODE

RESONANCE CONDITION

$$k_\beta < \frac{k_B}{2} < k_{\beta 0} \longrightarrow k_s < \frac{k_L}{2} < k_{s0}$$

ADDITIONAL COMPLICATION:

INTRINSIC NON-LINEARITY OF rf BUCKET

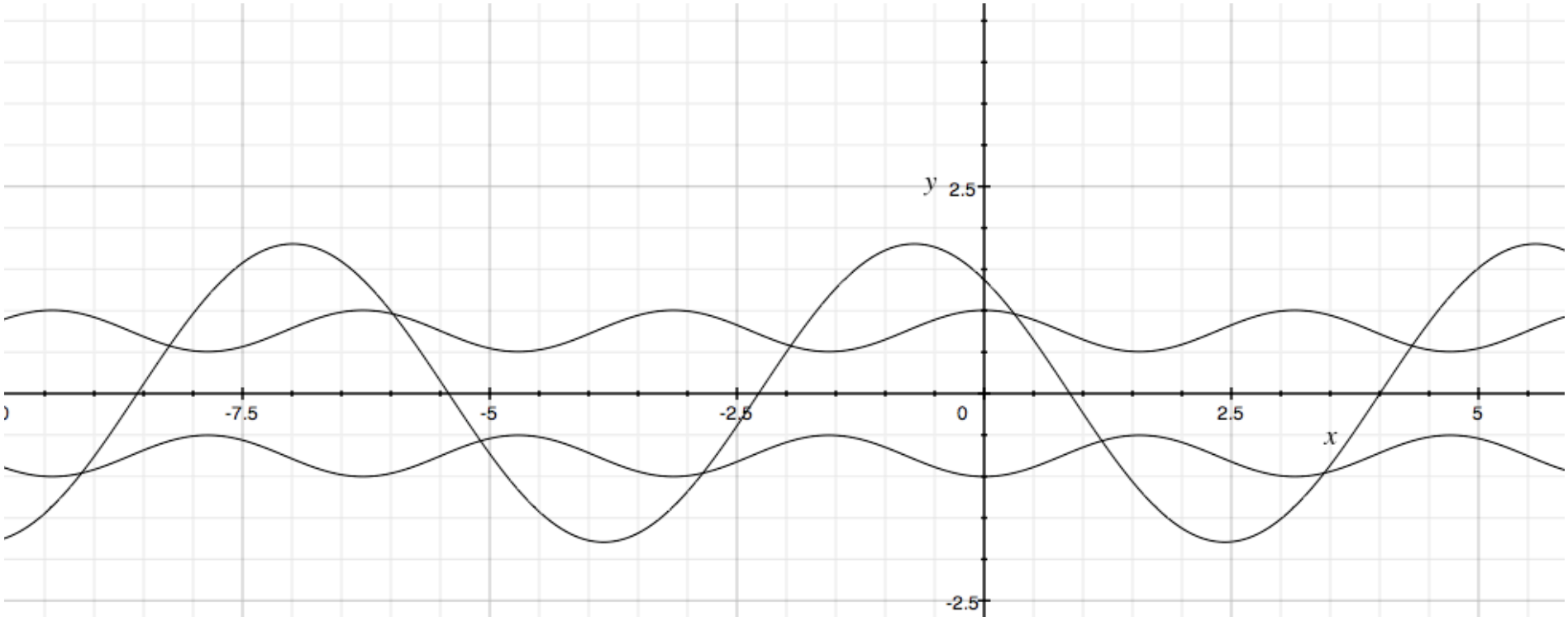

Particle frequency = (1/2) Envelope frequency

As particle dives in and out of envelope, particle is at same phase of envelope oscillation.

Those particles that are exiting the beam when beam radius is small, and entering beam when beam radius is large, get larger "kick" going out and smaller kick coming in, so are driven to large amplitude.

FROM Tom Wangler
Los Alamos National Lab

Stroboscopic Map (The Peanut Diagram)

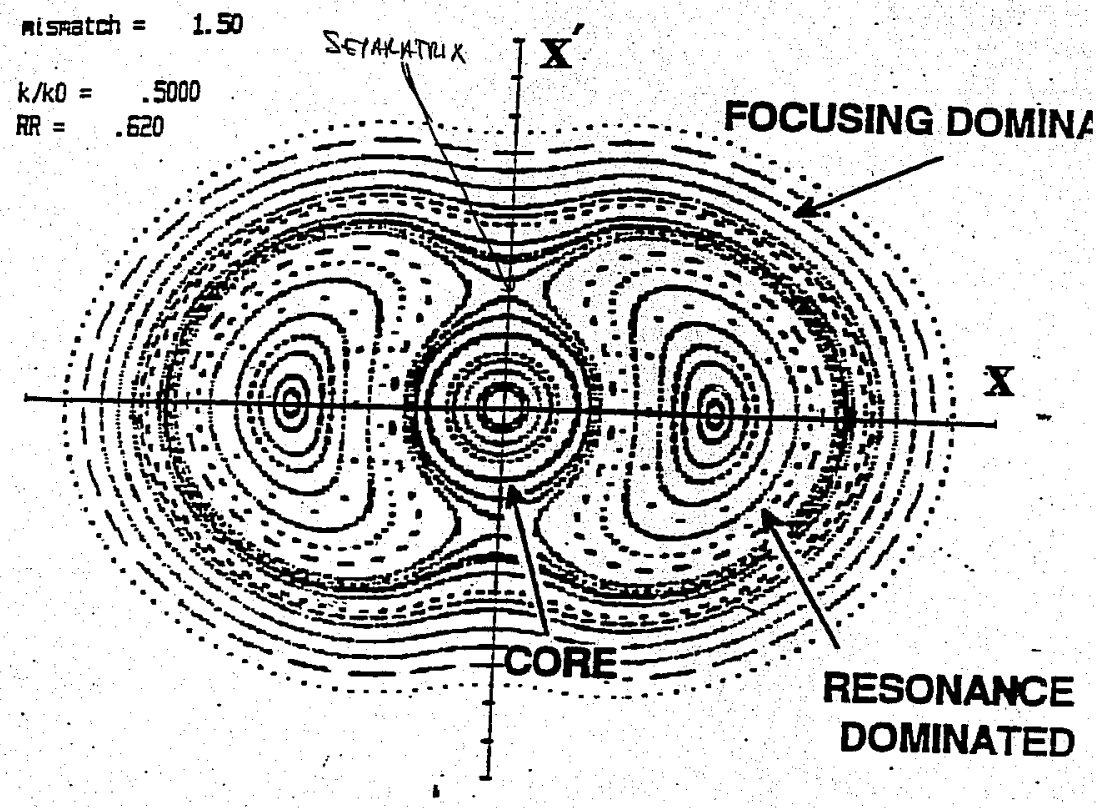

- **Accumulate Many Snapshots of Phase Space Taken at Minimum Amplitude of Core Oscillation.** (OR ANY PARTICULAR PHASE)
- **Follow an Array of Particles to Obtain a "Trajectory Field".**
- **Regular Trajectories Appear as Smooth Curves.**
- **Chaotic Trajectories Appear as Stochastic Scatter.**
- INITIAL POSITIONS OF PARTICLES IN PHASE SPACE WERE EQUALLY SPACED ALONG X & X' AXES.

Orbits of resonant particles have amplitudes which are highly varying compared to non-resonant particles

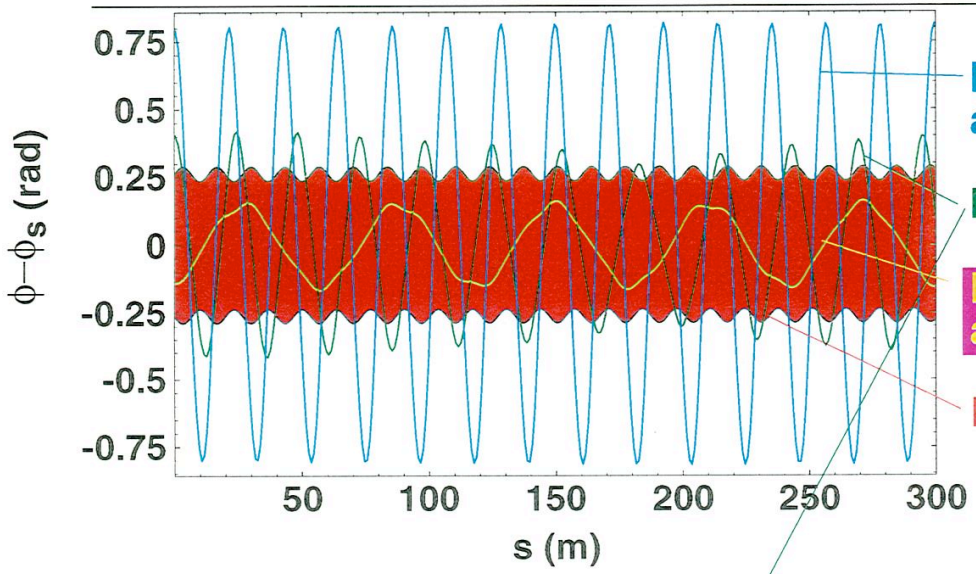

Oscillation frequency

Non-resonant large amplitude particle	$< k_{s0}$ (or $k_{\beta 0}$)
Resonant particle	$\sim k_L/2$ (or $k_{\varepsilon nv}/2$)
Non-resonant low amplitude particle	$\sim k_s$ (or k_β)
Beam envelope	k_L (or $k_{\varepsilon nv}$)

Poincare plot strobes phase space each envelope oscillation

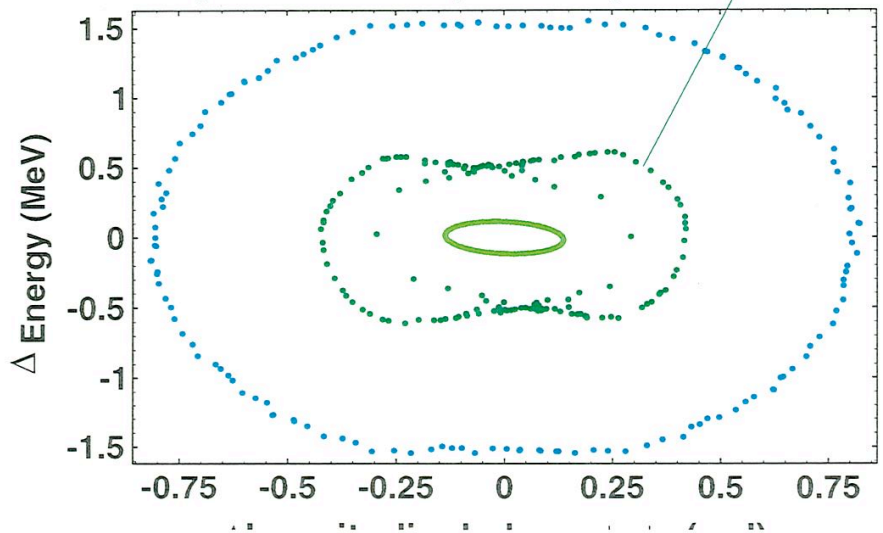

Note that resonant particle undergoes 11 oscillation periods, half of the 22 periods of the envelope. (The two non-resonant particles undergo 14 and 5 oscillation periods.)

Non-resonant large and small amplitude particles have regular orbits whereas resonant particles have varying amplitudes

Changing Poincare phase rotates diagram as expected

$k_L s = 0$

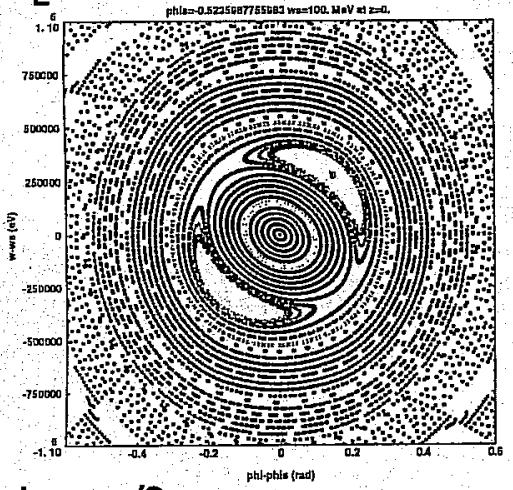

$k_L s = \pi/6$

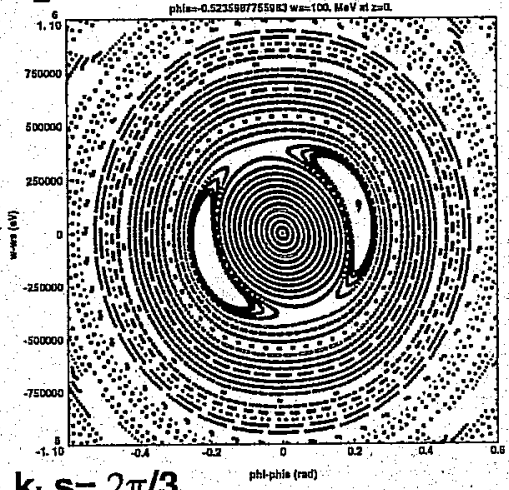

$k_L s = \pi/3$

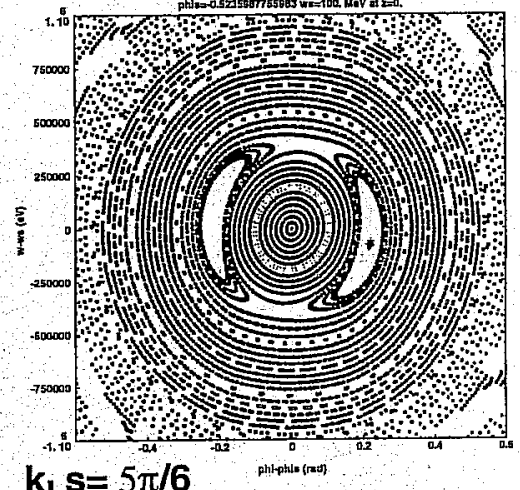

$k_L s = \pi/2$

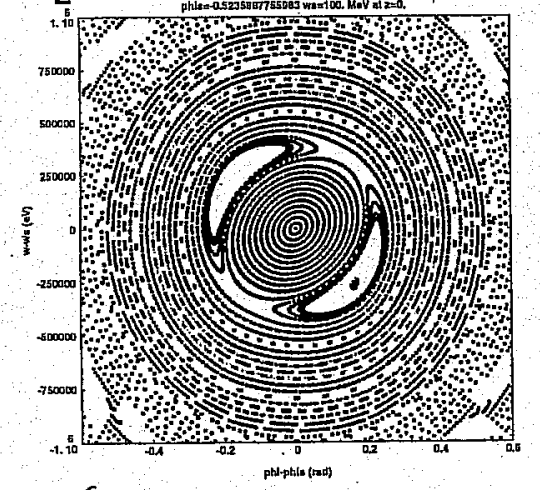

$k_L s = 2\pi/3$

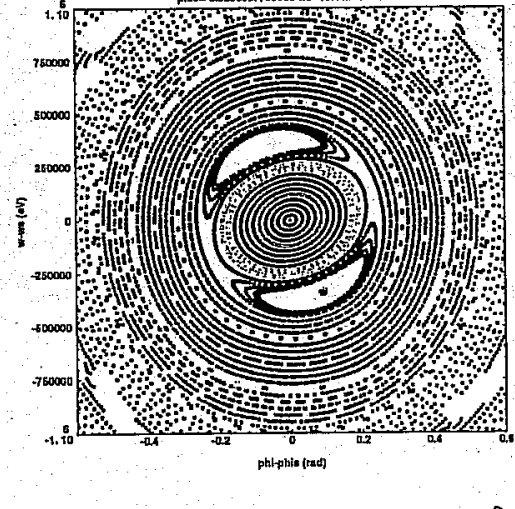

$k_L s = 5\pi/6$

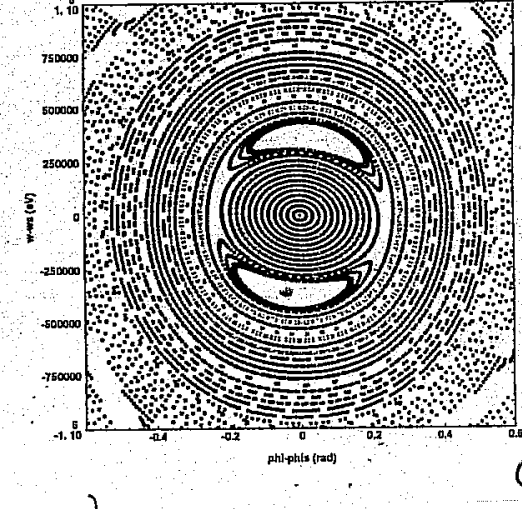

(CHANGING $k_L s$ by π ROTATES POINCARE PLOT BY π.)

$k_b^2/k_0^2 = 3 + \eta^2$ for the spherical bunch.

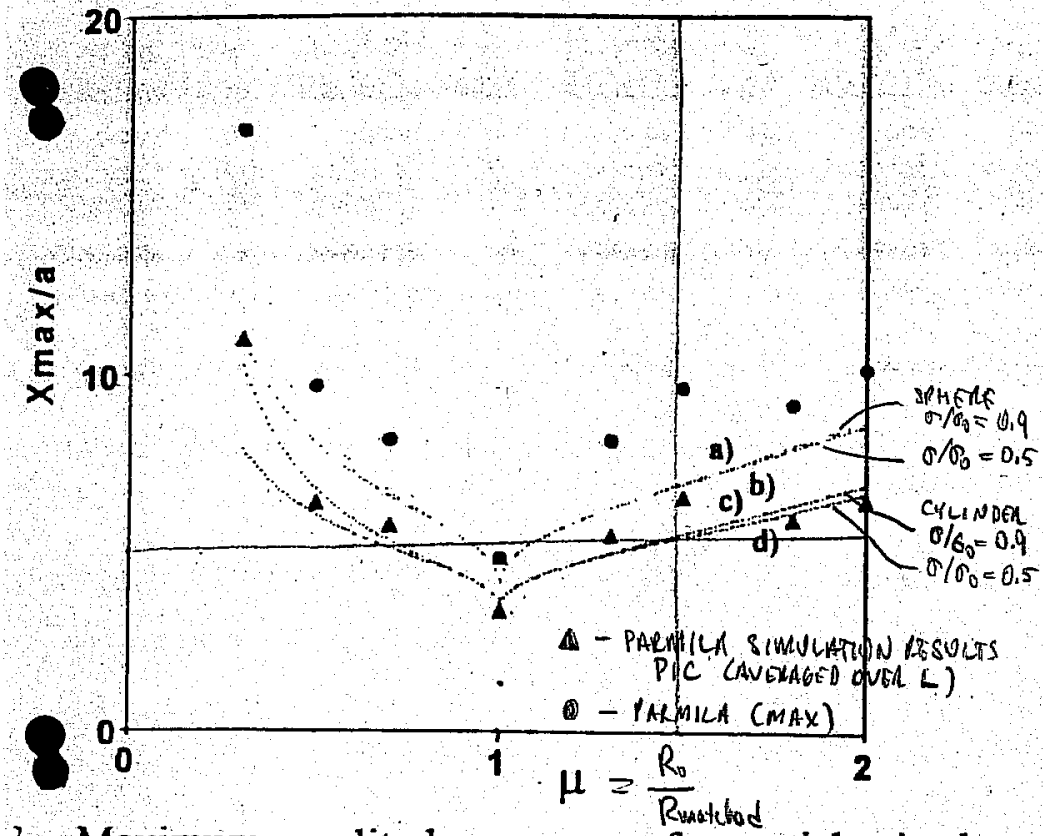

3. Maximum amplitudes versus μ for particles in the nance regions for the cylinder, and sphere models: a) re, $\eta = 0.9$, b) sphere, $\eta = 0.5$, c) cylinder, $\eta = 0.9$, and d) nder, $\eta = 0.5$. The triangles represent the smoothed MILA simulation results for comparison with the els, and the dots represent the maximum amplitudes ding quadrupole flutter.

a real linac, additional effects that are not included in the cle-core model, must be accounted for, such as beam-ope flutter associated with a quadrupole focusing system, eration, and the influence of other modes of the ai ned beam. We have conducted a test of the predictions ie particle-core model, by carrying out PARMILA ations, using an r-z space-charge mesh with individual

note that t
mesh to en
simulations

Work du
that beam
the new li
mainly resp
models to n
formed. Th
and one fo
limited to a
the strengt
predictions
bounds of t
a linac. Sin
produce sn
consistent v
that the brea
the halo. To
as well as
keeping ε s
can contrib
beam-resid
However, th
than beam n

The author
Gluckstern a

* Work supp

FROM WANGLER et al
XVIII Int'l LINAC CONF.
GENEVA, SWITZERLAND,
AUG. 26-30, 1996

WANGLER'S CORE/TEST PARTICLE RESULTS

$$\frac{X_{max}}{\langle x^2 \rangle^{1/2}} = A + B|\ln \mu| \qquad \mu = \left(\frac{r_{bi}}{r_{bo}}\right)$$

$= \frac{\text{INITIAL BEAM RADIUS}}{\text{MATCHED BEAM RADIUS}}$

FOR	%	A	B
CYLINDER	0.5	3.97	3.83
CYLINDER	0.9	3.91	4.25
SPHERE	0.5	4.87	5.30
SPHERE	0.9	4.81	5.56

Numerical Validation of 1D particle-core model

- Maximum beam size in large scale simulations found to be in excellent agreement with "peanut diagram" of particle-core model

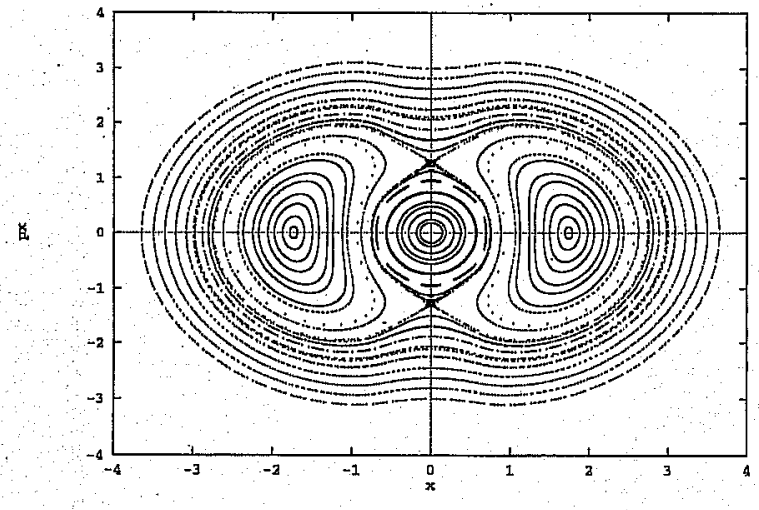

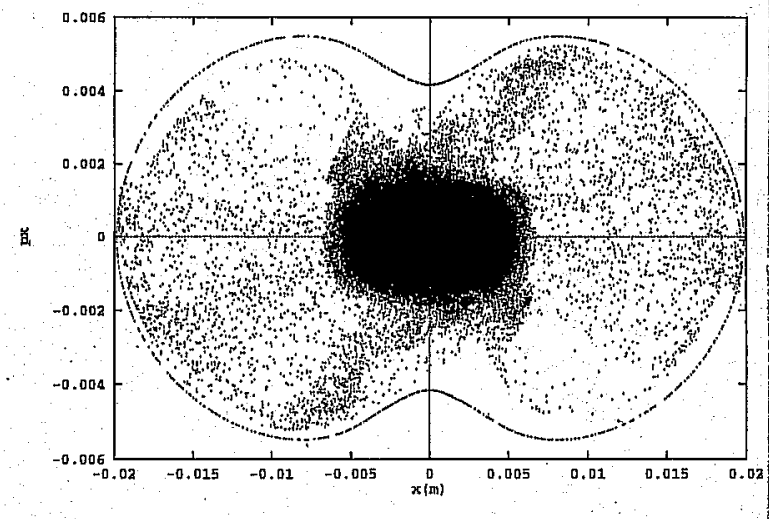

Longitudinal Particle-Core Model w/ RF Nonlinearity

- Core-Test-Particle (CTP) code
  exhibits asymmetry in peanut diagram also observed in simulations with HALO3D PIC code
- 200 mA simulation:

CTP test particles

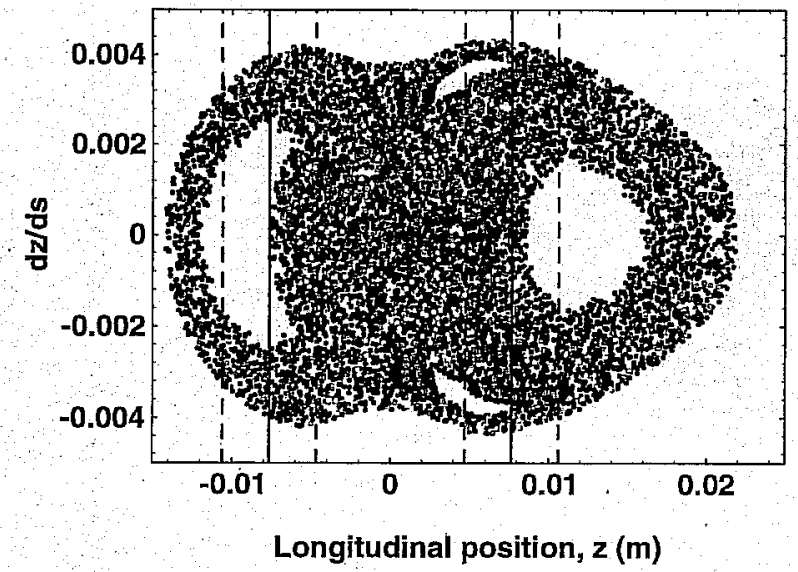

HALO3D beam particles

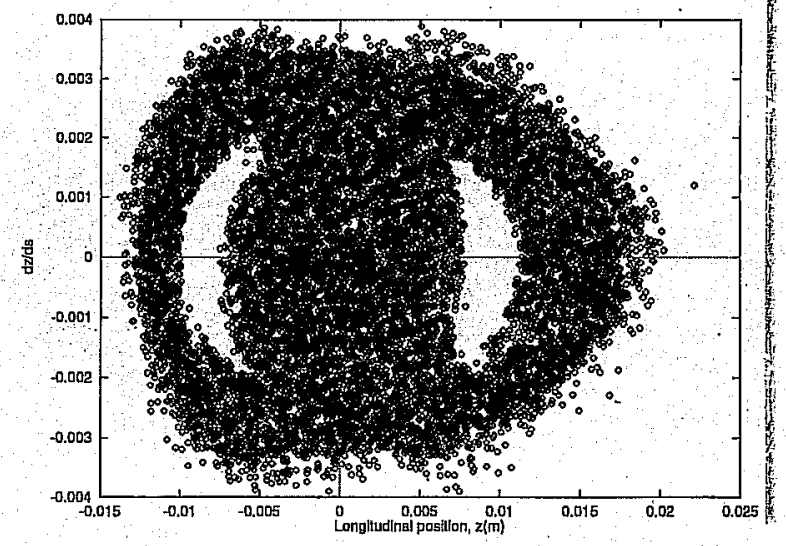

Longitudinal Particle-Core Model w/ RF Nonlinearity

- Absence of $k_L/2$ resonance (and associated halo) predicted by CTP analysis confirmed in HALO3D simulations
- 5 mA simulation:

CTP test particles

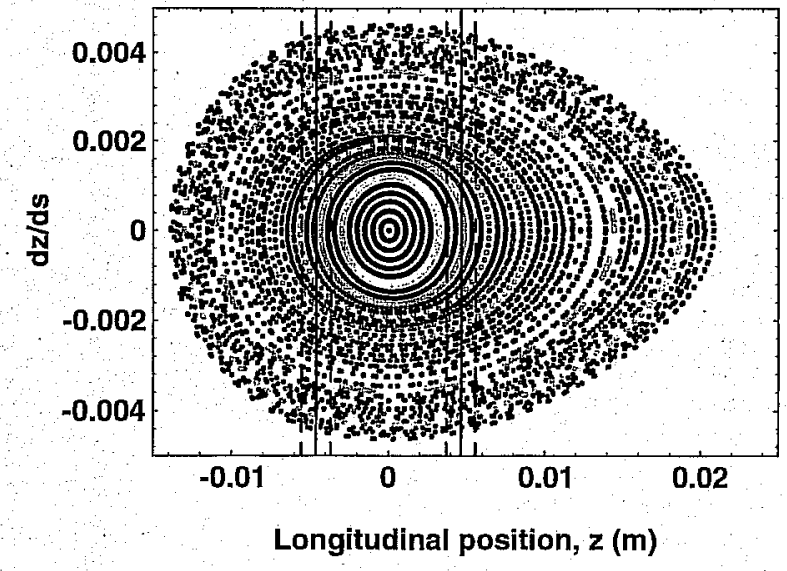

HALO3D test particles

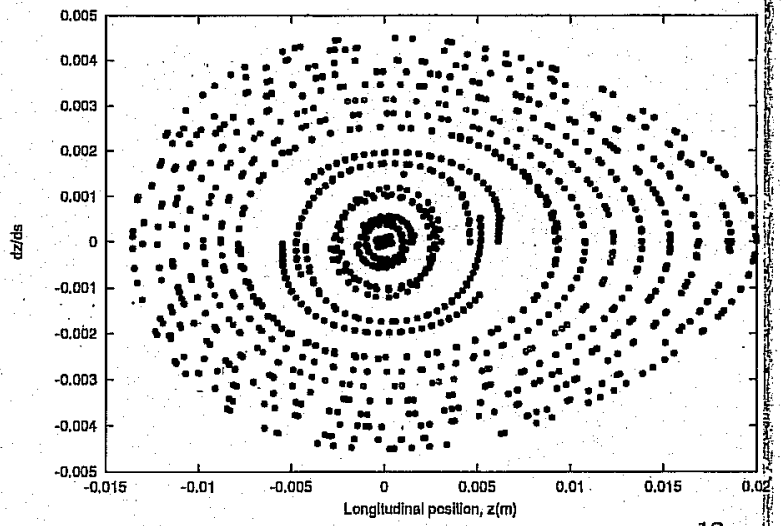

Model w/out RF Nonlinearity

- $k_L/2$ resonance present in 5 mA CTP run when nonlinearity is turned off. Also observed in HALO3D.

CTP test particles

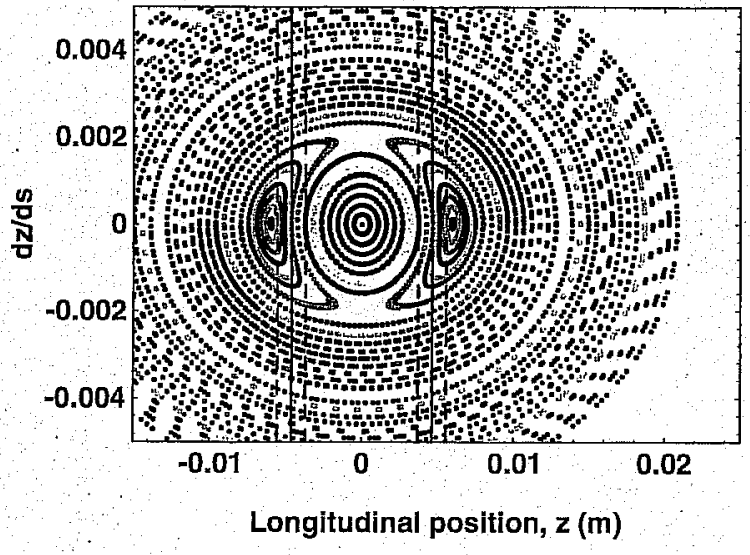

HALO3D test particles

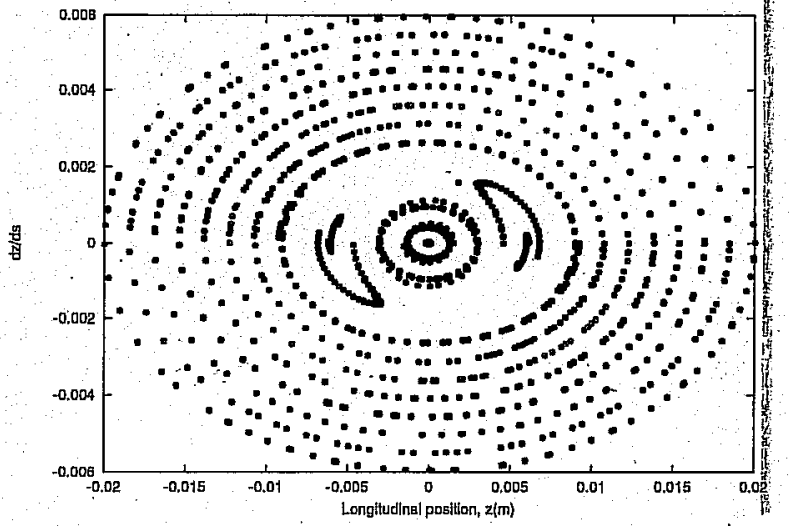

Numerically determined frequency and amplitude of particle oscillations: linear rf focusing

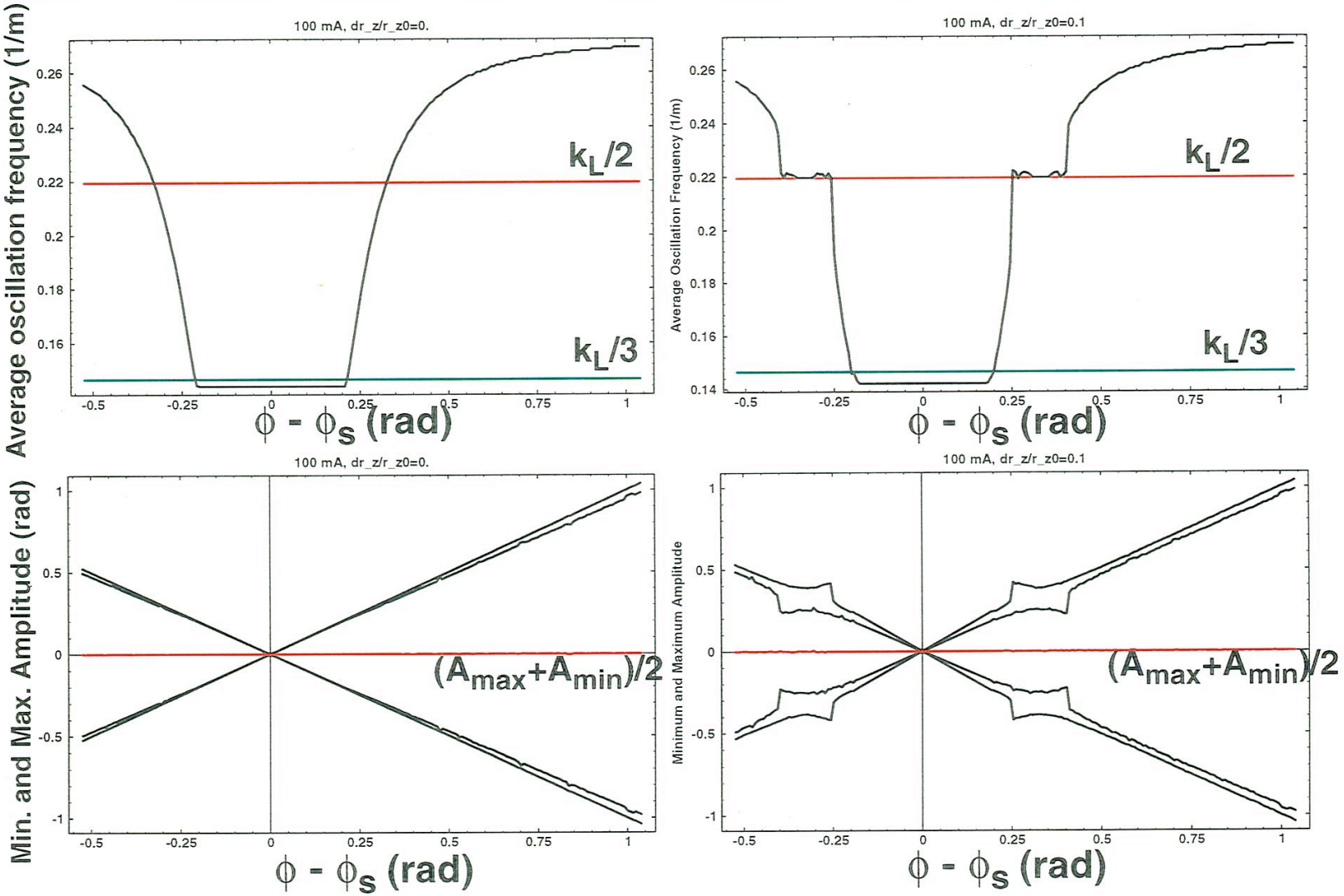

Numerically determined frequency and amplitude of particle oscillations: non-linear rf focusing

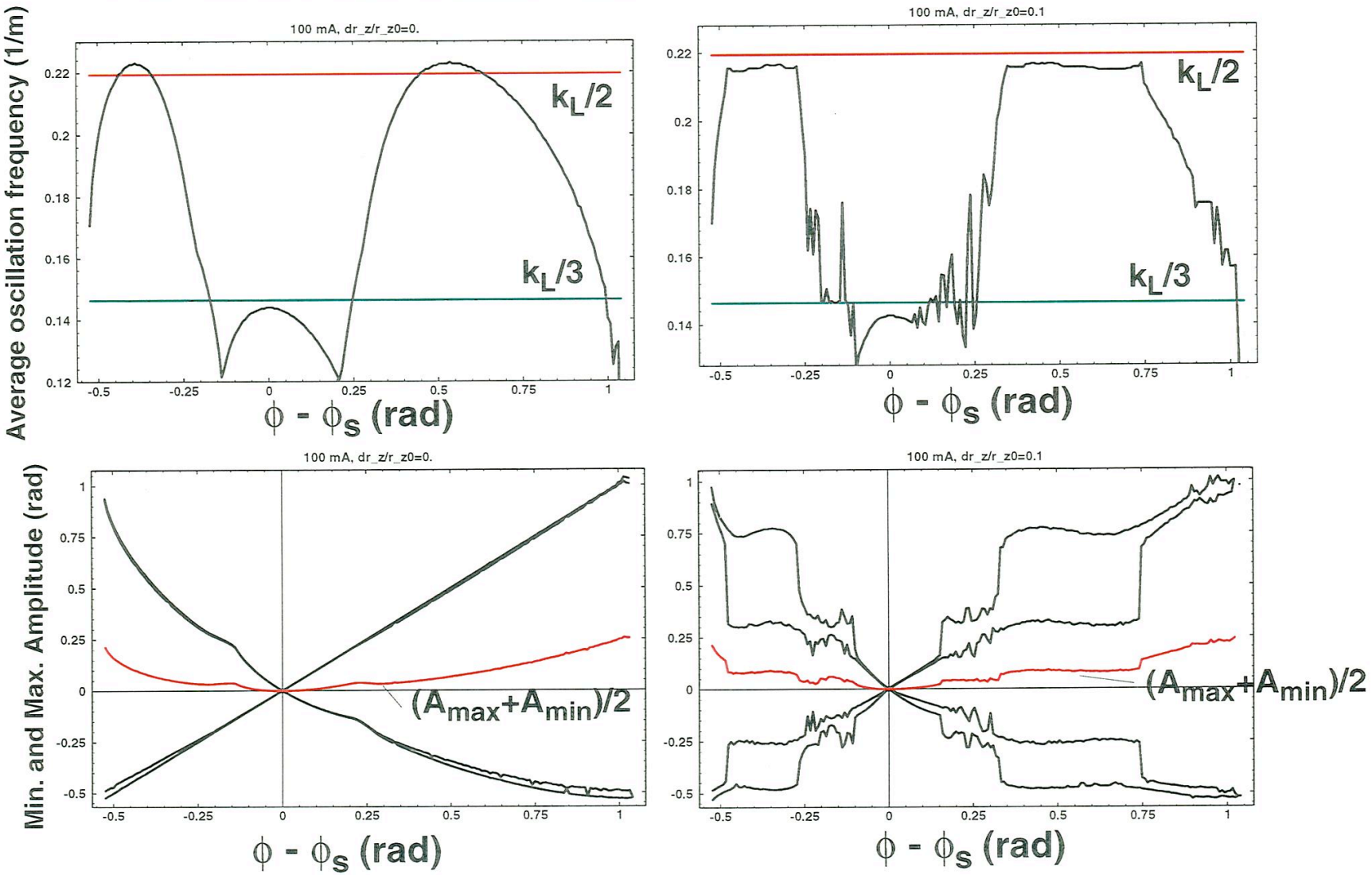

For non-linear rf, $k_L/2$ resonance occurs only over a range of current

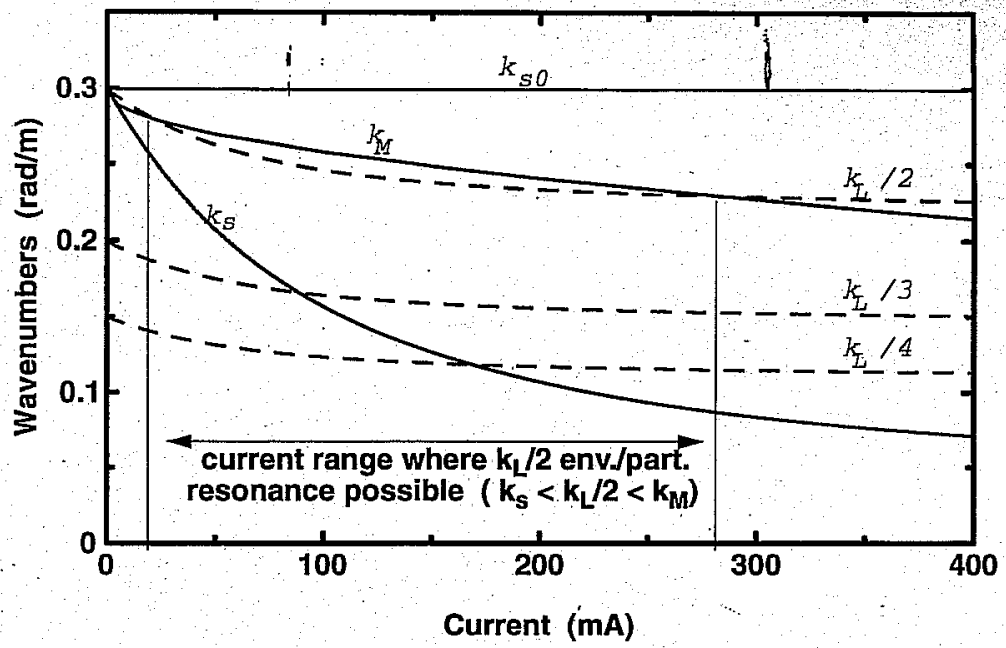

k_{s0} = single particle frequency

k_s = space-charge depressed synchrotron frequency

k_M = maximum particle oscillation frequency

k_L = longitudinal envelope oscillation frequency

AMPLITUDE PHASE ANALYSIS

GLUCKSTERN, PHYS. REV. LETTERS 73, 1247 1994

$$x'' + k_{\rho 0}^2 x = \begin{cases} \frac{Q}{r_b^2} x & \text{for } r < r_b \\ \frac{Q}{r^2} x & \text{for } r > r_b \end{cases}$$

Assume $r_b = r_{b0} + \epsilon \cos(k_B s)$

$$x'' + k_\rho^2 x = \overbrace{-\frac{Q}{r_{b0}^2} x\left(1 - \frac{r_{b0}^2}{r^2}\right) H(r - r_{b0})}^{\text{EXTERIOR}} + \overbrace{\frac{2\epsilon Q}{r_{b0}^2} x \cos k_B s \, H(r_{b0} - r)}^{\text{INTERIOR}}$$

$H(x) = \begin{cases} 1 & x > 0 \\ 0 & x < 0 \end{cases}$

NON-LINEAR TERM MAKES AMPLITUDE DEPENDENT FREQUENCY

ARISING SOLELY FROM ENVELOPE PERTURBATION; ALLOWS TRANSFER FROM CORE

$$k_\rho^2 \equiv k_{\rho 0}^2 - \frac{Q}{r_{b0}^2}$$

GLUCKSTERN TREATED GENERAL CASE OF ARBITRARY ANGULAR MOMENTUM. FOR ILLUSTRATION HERE I SET ANG. MOM = 0. $\Rightarrow x = r$

USE PHASE AMPLITUDE METHOD

$$\frac{x}{r_{b0}} \equiv A(s) \sin\psi(s) \qquad \psi \equiv k_\rho s + \alpha(s)$$

$$\frac{x'}{r_{b0}} \equiv k_\rho A(s) \cos\psi(s)$$

k_ρ: OSCILLATION AT DEFLECTED PHASE ADVANCE

α: SLOWLY CHANGING PHASE

Let $x'' + k_\rho^2 x = f(x, s)$

$= f(A, \psi, k_B s)$

NOTE $\frac{x'}{r_{b0}} = A' \sin\psi + (k_\rho + \alpha') A \cos\psi$

$= k_\rho A \cos\psi$

$\Rightarrow A' \sin\psi + \alpha' A \cos\psi = 0$

$\frac{\partial}{\partial s}$ A & $\frac{\partial}{\partial s}\alpha$ CAN BE EXPRESSED IN TERMS OF f

$$x'' = k_\beta r_{b0} A' \cos\psi - k_\beta r_{b0} A \sin\psi \underbrace{(k_f + \alpha')}_{\psi'}$$

$$+ k_\beta^2 x = k_f^2 r_{b0} A \sin\psi$$

$$x'' + k_\beta^2 x = k_f r_{b0} A' \cos\psi - k_\beta r_{b0} A \sin\psi\, \alpha' = f(\alpha, \delta)$$

ALSO $A' \sin\psi + A \cos\psi\, \alpha' = 0$

$$\begin{bmatrix} k_\beta r_{b0} \cos\psi & -k_\beta A r_{b0} \sin\psi \\ \sin\psi & A\cos\psi \end{bmatrix} \begin{bmatrix} A' \\ \alpha' \end{bmatrix} = \begin{bmatrix} f \\ 0 \end{bmatrix}$$

INVERTING MATRIX:

$$\begin{bmatrix} A' \\ \alpha' \end{bmatrix} = \frac{1}{A k_\beta r_{b0}} \begin{bmatrix} A\cos\psi & k_\beta A r_{b0} \sin\psi \\ -\sin\psi & k_f r_{b0} \cos\psi \end{bmatrix} \begin{bmatrix} f \\ 0 \end{bmatrix}$$

$$A' = \frac{\cos\psi}{k_f r_{b0}} f$$

$$\alpha' = \frac{-\sin\psi}{k_f r_{b0} A} f$$

USING THESE DEFINITION THE EQUATION OF MOTION CAN BE EXPRESSED AS:

$$A' = \frac{1}{k_p r_{b0}} f(A, \psi, k_B s) \cos\psi$$

$$\alpha' = \frac{-1}{k_p A r_{b0}} f(A, \psi, k_B s) \sin\psi$$

At resonance we expect $2k_p - k_B \sim 0$,

so define $\Psi = 2\psi - k_B s = (2k_p - k_B)s + 2\alpha$

$$\Rightarrow \Psi' = (2k_p - k_B) + 2\alpha'$$

ELIMINATE $k_B s$ in $f(A, \psi, k_B s)$ using

$$k_B s = 2\psi - \Psi$$

AVERAGE OVER ALL NON-RESONANT FREQUENCY COMPONENTS, FOR RESONANT PARTICLE EQUATIONS OF MOTION:

$$A_r' = \frac{1}{k_p r_{b0}} \int_{-\pi}^{\pi} \frac{d\psi}{2\pi} f(A_r, \Psi_r, \psi) \cos\psi$$

$$\alpha_r' = \frac{-1}{r_{b0} k_p A_r} \int_{-\pi}^{\pi} \frac{d\psi}{2\pi} f(A_r, \Psi_r, \psi) \sin\psi$$

A_r & $\Psi_r = (2k_p - k_B)s + 2\alpha$ are held fixed during integration.

THE RESULT IS

$$A_r' = F_1(A_r, \Psi_r)$$

$$\Psi_r' = (2k_p - k_B) + 2F_2(A_r, \Psi_r)$$

where F_1 & F_2 are explicit functions of A_r & Ψ_r

Let $\omega = A_r^2$

$$\omega' = 2A_r A_r' = 2A_r F_1(A_r, \Psi_r) = 2\omega^{1/2} F_1(\omega^{1/2}, \Psi_r)$$

$$\Psi' = (2k_p - k_B) + 2F_2(A_r, \Psi_r)$$

ω & Ψ are conjugate variables, and the resonant particle equation of motion can be derived from an s-independent Hamiltonian H as:

$$\omega' = \frac{\partial H}{\partial \Psi} \qquad \Psi' = -\frac{\partial H}{\partial \omega}$$

GLUCKSTERN FOUND A CONSTANT OF THE MOTION $H_r(\omega, \Psi)$ which satisfies Hamilton's EQUATIONS.

RESONANT PARTICLE WOULD STAY ON LINES OF CONSTANT H.

GLUCKSTERN'S SIMPLIFIED EXAMPLE

$$x'' + k_\beta^2 x = -\frac{Q}{r_{bo}^4} x^3 + \frac{zeQ}{r_{bo}^2} x \cos k_\beta s$$

↑ NON-LINEAR FORCE

↑ OSCILLATING CORE

THIS example:

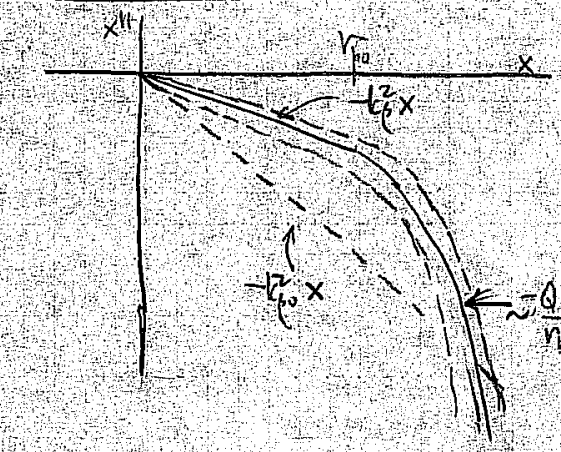

ACTUAL MODE OF BREATHING BEAM

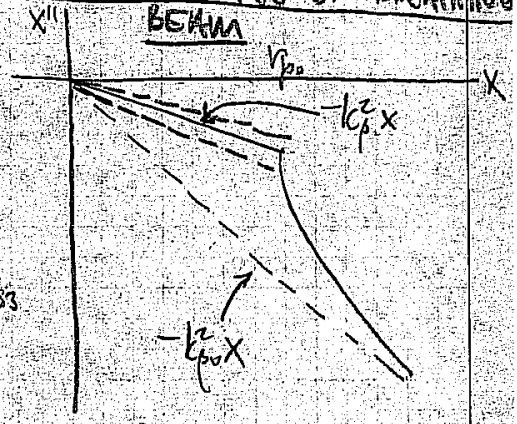

$$x'' + k_\beta^2 x = -\frac{Q}{r_{bo}^4} x^3 + \frac{2\epsilon Q}{r_{bo}^2} x \cos k_\beta s$$

$$\equiv f(x,s)$$

$$= -\frac{Q}{r_{bo}} A^3 \sin^3\psi + \frac{2\epsilon Q}{r_{bo}} A \sin\psi \cos k_\beta s$$

$$\left(\text{where } \frac{x}{r_{bo}} \equiv A\sin\psi \;\&\; \frac{x'}{r_{bo}} \equiv k_\beta A \cos\psi\right)$$

$$\Rightarrow A' = \frac{\cos\psi}{k_\beta r_{bo}} f = -\frac{Q}{k_\beta r_{bo}^2} A^3 \sin^3\psi\cos\psi + \frac{\epsilon Q}{k_\beta r_{bo}^2} A \sin 2\psi \cos k_\beta s$$

$$\alpha' = \frac{-\sin\psi}{k_\beta r_{bo} A} f = \frac{Q}{k_\beta r_{bo}^2} A^2 \sin^4\psi + \frac{2\epsilon Q}{k_\beta r_{bo}^2} \sin^2\psi \cos k_\beta s$$

Using $\Psi \equiv 2\psi - k_\beta s \Rightarrow \cos k_\beta s = \cos[2\psi - \Psi]$

$$= \cos[2\psi]\cos[\Psi] + \sin[2\psi]\sin[\Psi]$$

TRIG IDENTITIES:

$$\sin 2\psi \cos k_\beta s = \frac{1}{2}\sin\Psi - \frac{1}{2}\cos 4\psi \sin\Psi + \frac{1}{2}\sin 4\psi \cos\Psi$$

$$\sin^4\psi = \frac{3}{8} - \frac{1}{2}\cos 2\psi - \frac{1}{8}\cos 4\psi$$

$$\sin^2\psi \cos k_\beta s = \cos\Psi\left[-\frac{1}{4} + \frac{1}{2}\cos 2\psi - \frac{1}{4}\cos 4\psi\right] + \sin\Psi\left[\frac{1}{2}\sin 2\psi - \frac{1}{4}\sin 4\psi\right]$$

$$\sin^3\psi\cos\psi = \frac{1}{4}\sin 2\psi - \frac{1}{8}\sin 4\psi$$

$$\Rightarrow A_r' = \frac{\epsilon Q}{2k_\beta r_{b0}^2} A_r \sin\Psi_r$$

$$\Psi_r' = (2k_\beta - k_B) + 2\alpha_r'$$

$$= (2k_\beta - k_B) + \frac{3Q}{4k_\beta r_{b0}^2} A_r^2 + \frac{\epsilon Q}{k_\beta r_{b0}^2} \cos\Psi$$

DEFINE $w = A_r^2$

$$w' = 2A_r A_r' = \frac{\epsilon Q}{k_\beta r_{b0}^2} w \sin\Psi_r$$

$$\Psi_r' = (2k_\beta - k_B) + \frac{3Q}{4k_\beta r_{b0}^2} w + \frac{\epsilon Q}{k_\beta r_{b0}^2} \cos\Psi$$

A Hamiltonian can be found satisfying Hamilton's equations:

$$-H = (2k_\beta - k_B) w + \frac{3}{2} \frac{Q}{k_\beta r_{b0}^2} w^2 + \frac{\epsilon Q}{k_\beta r_{b0}^2} w \cos\Psi$$

THIS CAN BE EXPRESSED AS:

$$\epsilon \cos\Psi = \Delta - \frac{3}{2} w - \frac{C}{w}$$

where C is determined by initial conditions and:

$$\Delta = k_\beta (k_B - 2k_\beta) r_{b0}^2 / Q$$

(NOTE: $k_B^2 = 4k_\beta^2 + 2Q/r_{b0}^2$ for breathing mode).

. (2.4) and (2.5)

$\cos pz]$, (2.5)

:]. (2.6)

oscillatory terms
number $2q - p$

(2.7)

os Ψ, (2.8)

of this resonant
al of the motion

, (2.9)

and where the
he initial values
pe equation we
breathing mode,

, (2.10)

d by the space

Guided by the parametrization of the x and
separately, the amplitude-phase parametrizati
two-dimensional oscillation is written as

$$s = \frac{w^2 + L^2}{2w} - \frac{w^2 - L^2}{2w}\cos(2qz + \gamma).$$

Here w and γ are slowly varying amplitude
parameters which would be constant if the rig
Eq. (2.11) vanished. We now write

$$s' = q\,\frac{w^2 - L^2}{w}\sin(2qz + \gamma)$$

and use Eq. (2.11) and the required connectio
w' and γ' implied by Eq. (2.13) to obtain explic
sions for w' and γ'. We then average over osci

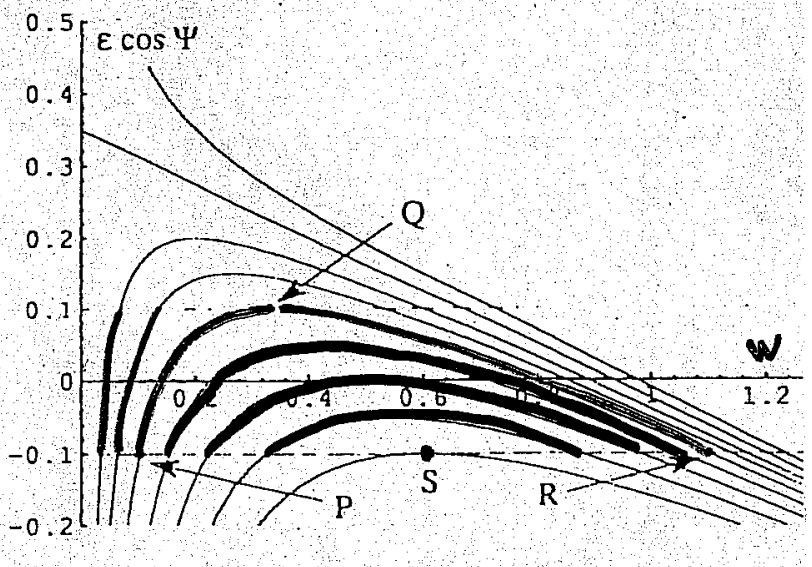

FIG. 1. Plot of $\epsilon\cos\Psi$ vs w for the simplified n
$\Delta = 0.35$.

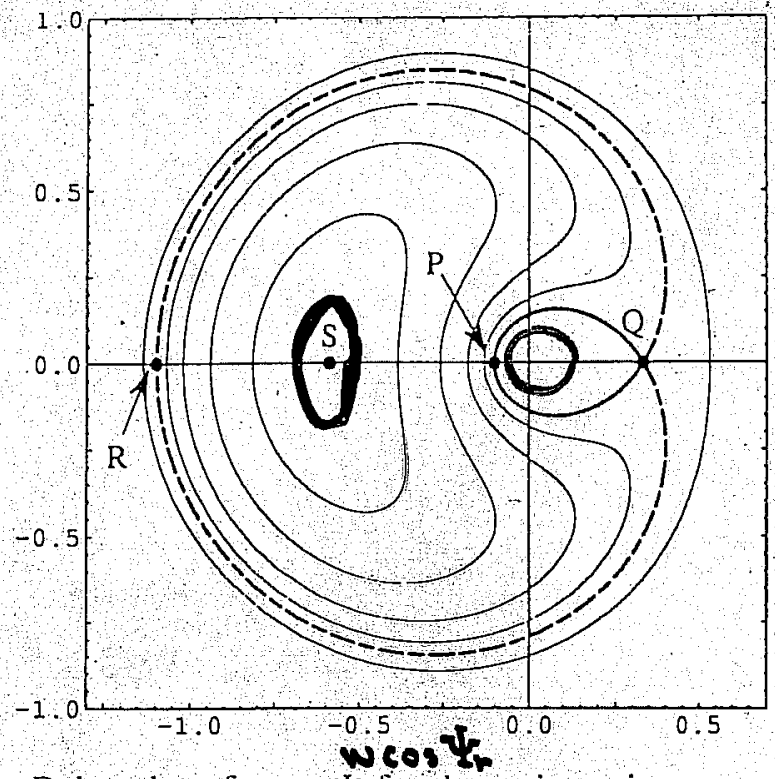

FIG. 2. Polar plot of w vs Ψ for the trajectories corresponding to the parametric resonance using $\Delta = 0.35$, $\epsilon = 0.1$, and the simplified model.

all wave numbers except $2q - p$, being careful to include the step functions as we obtain these averages. The final equations for w' and Ψ' [$\Psi = (2q - p)z + \gamma$] are similar to Eqs. (2.7) and (2.8) and again lead to an integral of the motion, which now is

$$g(1 - h)\epsilon \cos\Psi = f\Delta - t - C, \qquad (2.14)$$

where $f(w) = (w^2 + L^2)/2w$, $g(w) = (w^2 - L^2)/2w$.

Here

^{2} (2.15)

Also

$\overline{f}$)

(2.16)

The arc-
quadrant.
ependence
ression for
; Eq. (2.6)

fect when
rough the
$\Delta = 0.35$
ry similar
Fig. 4 for
model in
cale for w
ming with
en by the

m.—The
to

Therefore the distribution in L for a K-V beam is unif
from $L = -1/2$ to $L = 1/2$ and vanishes for $|L| > 1/$

IV. Implications of the model.—Since the bread
K-V beam is a solution of the Vlasov equation, parti
within the core will continue to remain there, ever
the presence of the resonant interaction. If howe

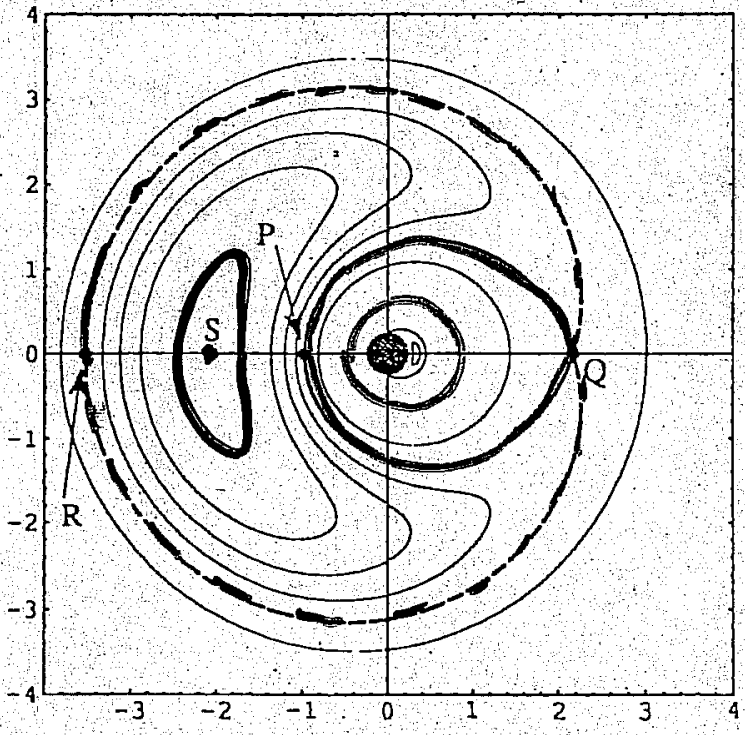

FIG. 4. Polar plot of w vs Ψ for the trajectories correspon
to the parametric resonance using $\Delta = 0.35$, $L = 0$, $\epsilon =$
and the exact model.

Bob Gluckstern
Univ. of Maryland.

$$x = \pm 3^{1/2} r_0 \sin\left[\frac{\theta_0 + 2\theta}{2}\right]^2$$

$$x' = \pm 3^{1/2} r_0 k_0 \cos\left[\frac{\theta_0 + 2\theta}{2}\right]^2$$

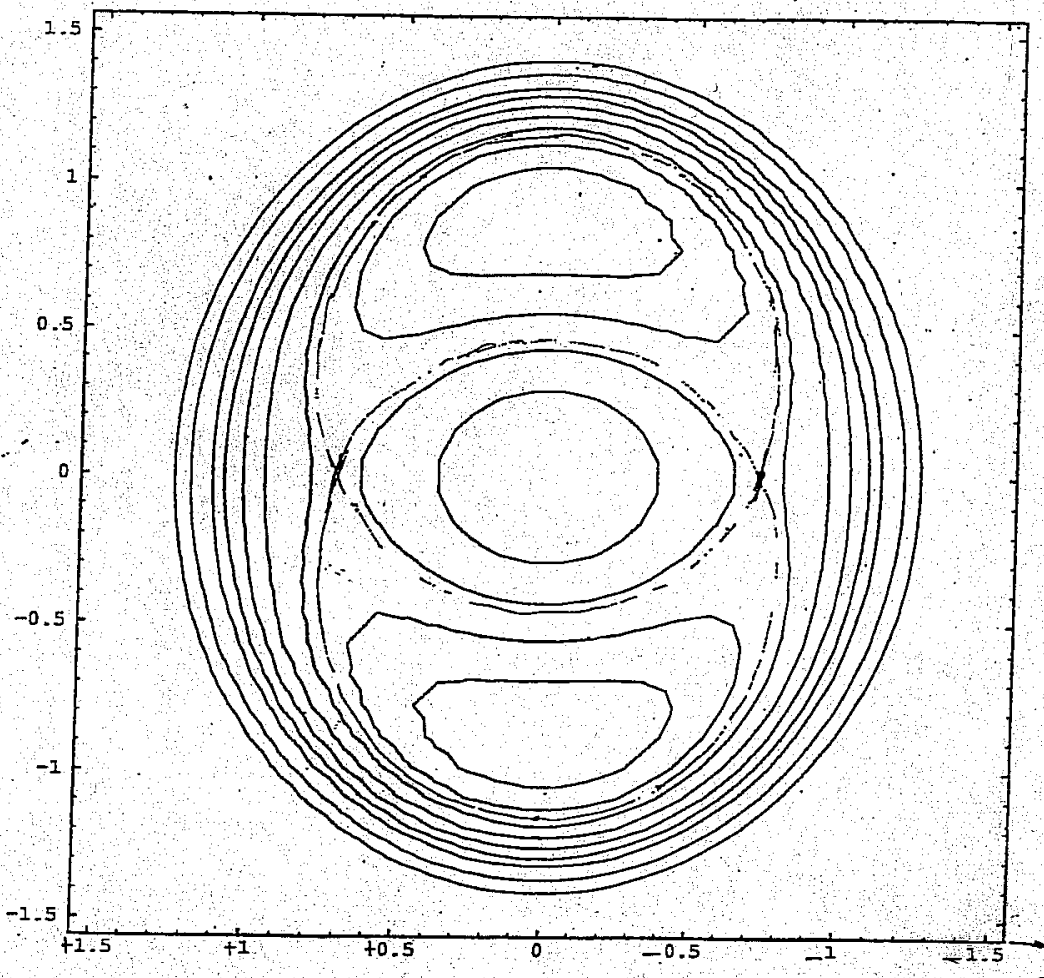

$x'/\beta a$

$x/\beta a$ (scaled)

x' (scaled)

Fig 3.

From Tom Wangler
Los Alamos National Lab

Stroboscopic Map (The Peanut Diagram)

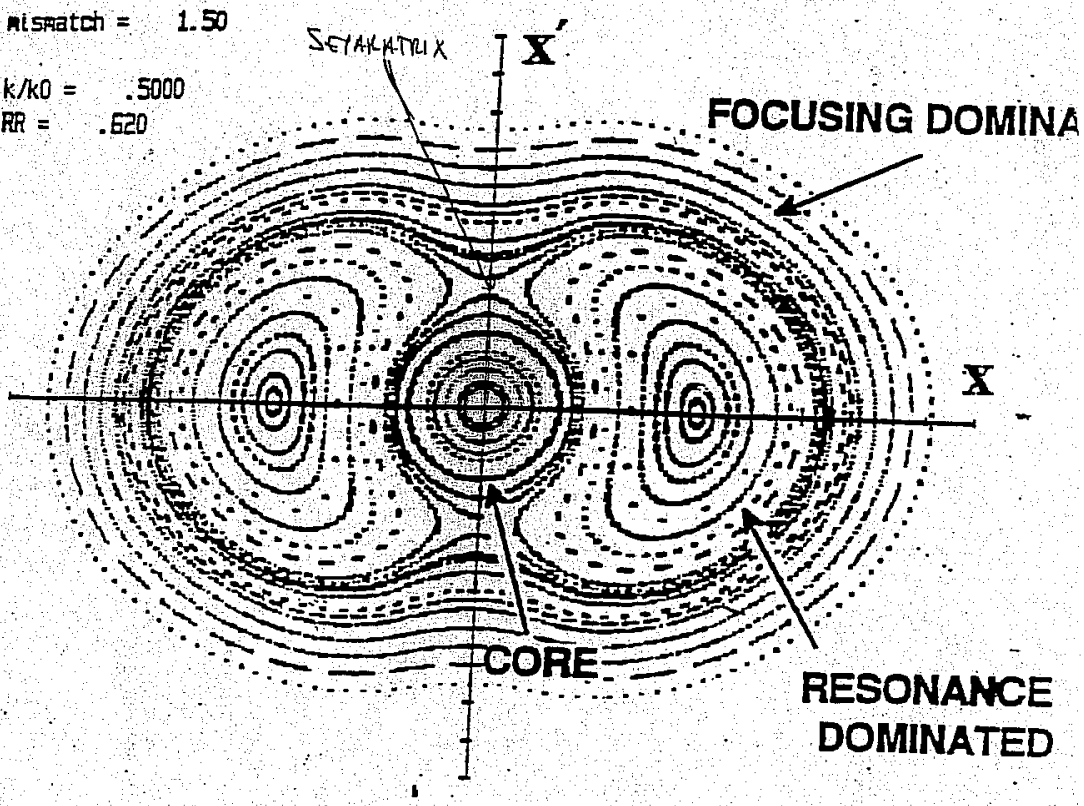

- **Accumulate Many Snapshots of Phase Space Taken at Minimum Amplitude of Core Oscillation.** (OR ANY PARTICULAR PHASE)
- **Follow an Array of Particles to Obtain a "Trajectory Field".**
- **Regular Trajectories Appear as Smooth Curves.**
- **Chaotic Trajectories Appear as Stochastic Scatter.**
- INITIAL POSITIONS OF PARTICLES IN PHASE SPACE WERE EQUALLY SPACED ALONG X & X' AXES.

Analytic Model for Halo Formation in High Current Ion Linacs

Robert L. Gluckstern

Physics Department, University of Maryland, College Park, Maryland 20742

(Received 8 March 1994)

We construct an azimuthally symmetric 2D model for halo formation in high current ion linacs. The driving term, a "breathing" oscillation caused by a transverse mismatch along the linac, leads to growth of ion amplitudes in the core through the parametric resonance. As the ion amplitude grows, its wave number increases, enhancing the resonance. This leads to the formation of a halo surrounding the core. We explore the dependence of this mechanism on the tune depression and the size of the mismatch. The model agrees well with simulations at Los Alamos, but does not yet include the effects of chaos observed in the simulations as the tune depression becomes severe.

PACS numbers: 41.85.−p, 29.17.+w, 29.27.Bd

I. Introduction.—High current, high duty factor ion linacs have become increasingly attractive in recent years. Among possible applications are heavy ion drivers for thermonuclear energy production, production of tritium, transmutation of radioactive wastes, and production of radioactive isotopes for medical use.

Obviously, it is desirable to accelerate the maximum possible current in such linacs. Much work has been done to explore the optimum transverse phase space distribution in such beams. In particular, the Kapchinsky-Vladimirsky (K-V) distribution [1] is simplest to analyze, since this projection into real space has a uniform density and therefore linear space charge forces. The stability of the K-V distribution has been analyzed and approximately confirmed by numerical simulations. Nevertheless it appears that, particularly at high currents, the K-V and other equilibrium distributions evolve to ones with rounded edges and tails. In many cases involving high peak current, the distribution spins off a cluster of particles in the form of a halo surrounding a dense core. This halo is seen in simulations as well as in actual linacs, such as LAMPF [2]. And efforts to remove the halo by collimation have been largely unsuccessful since the halos almost always regenerate.

It is clear that the halos will produce unacceptably high levels of radioactivity in high current, high duty factor linacs. For this reason considerable effort has recently been devoted to exploring their detailed structure and understanding the mechanism or mechanisms by which the halos are produced [3–6]. What has been learned is that halos are most likely to be produced at transition locations, such as where there are discontinuities in frequency, structure geometry, transverse focusing pattern, accelerating gradient and phase, etc.

In the present paper, we propose an analytic model for halo formation which appears to reproduce the main features seen in simulations and in actual linacs. In particular we consider a circular cw beam with a K-V core distribution and explore the motion of individual ions passing through the core. Since energy transfer between ions and the core can take place only if the core has a time dependent behavior, we consider the driving mechanism to be a "breathing" oscillation of the core. We then explore the resonant (parametric) interaction between the breathing core and the ions oscillating about and through the core. Of particular importance is the dependence of the frequency of each oscillating ion on its amplitude, which is related to the fraction of the oscillation for which the ion is within the core.

In spite of the fact that the actual distribution will have nonlinear fields, the use of a K-V distribution for the analysis leads us to a very likely mechanism for the development of the halo. In particular, the results provide an explanation for the low density region around the core which is surrounded by a somewhat higher density halo ring. This explanation will probably still apply for other self-consistent distributions.

II. Model.—We consider an azimuthally symmetric K-V core of radius a for which the equation of motion of an ion is

$$x'' + k^2 x = x\begin{Bmatrix} \kappa/a^2, & r \le a \\ \kappa/r^2, & r \ge a \end{Bmatrix}, \tag{2.1}$$

where the prime stands for d/dz, and k is the wave number of the transverse motion in the absence of space charge. The perveance of the beam, $\kappa = eI/2\pi\epsilon_0 m v^3$, is a dimensionless parameter proportional to the current I, where e, m, and v are the charge, mass, and ion velocity, and ϵ_0 is the permittivity of free space. The equation for y is identical to Eq. (2.1).

We now assume a core oscillation of wave number p of the form $a \to a(1 - \epsilon\cos pz)$ and expand a^{-2} in Eq. (2.1) to first order in ϵ, the relative oscillation amplitude. After some algebra, Eq. (2.1) can be written as

$$x'' + q^2 x = -\frac{\kappa}{a^2} x\left(1 - \frac{a^2}{r^2}\right)\Theta(r - a) + \frac{2\epsilon\kappa}{a^2} x\cos pz\,\Theta(a - r), \tag{2.2}$$

where $\Theta(u) = 1,0$ for $u > 0, u < 0$ and where $q = \sqrt{k^2 - \kappa/a^2}$ is the wave number of oscillations within the core.

0031-9007/94/73(9)/1247(4)$06.00

With the radial forces of Eq. (2.2), we see that the angular momentum $Lqa^2 \equiv xy' - x'y = r^2\theta'$ is constant. The equation for radial motion then becomes

$$r'' + q^2\left(r - \frac{L^2a^4}{r^3}\right) = -\frac{\kappa}{a^2}r\left(1 - \frac{a^2}{r^2}\right)\Theta(r-a) + 2\frac{\epsilon\kappa}{a^2}r\cos pz\,\Theta(a-r). \tag{2.3}$$

The first term on the right makes the oscillation wave number depend on amplitude and the second allows for energy transfer between the core and the oscillating ion.

In order to understand the role of the different terms in Eq. (2.3), we construct a simplified model by setting $L = 0$ and invoking a pendulum model for the first term on the right side of Eq. (2.3) by replacing $r(1 - a^2/r^2)\Theta(r-a)$ by r^3/a^2, corresponding to the cubic nonlinear term for a pendulum. (However, its sign is opposite from the conventional pendulum since, in our model, the wave number *increases* with increasing amplitude.) In addition, we extend the driving term to all values of r. The simplified equation for x is therefore

$$x'' + q^2x = -\frac{\kappa}{a^2}\frac{x^3}{a^2} + 2\frac{\epsilon\kappa}{a^2}x\cos pz. \tag{2.4}$$

We now use the phase-amplitude method by writing $x/a = A\sin\psi$, $x'/a = qA\cos\psi$, where $\psi = qz + \alpha$, implying $A'\sin\psi + A\alpha'\cos\psi = 0$. Here A and α are taken to be the slowly varying amplitude and phase parameters of the ion oscillation. Substituting into Eq. (2.4) and solving for A' and α' we obtain

$$A' = -\frac{\kappa A}{qa^4}[A^2\sin^3\psi\cos\psi - \epsilon a^2\sin 2\psi\cos pz], \tag{2.5}$$

$$\alpha' = \frac{\kappa}{qa^4}[A^2\sin^4\psi - 2\epsilon a^2\sin^2\psi\cos pz]. \tag{2.6}$$

We now average over all rapidly varying oscillatory terms with the exception of the one with wave number $2q - p$ (the parametric resonance) and obtain

$$A' = \frac{\epsilon\kappa}{2qa^2}A\sin\Psi, \tag{2.7}$$

$$\Psi' = (2q - p) + \frac{3\kappa}{4qa^4}A^2 + \frac{\epsilon\kappa}{qa^2}\cos\Psi, \tag{2.8}$$

where $\Psi = (2q - p)z + 2\alpha$ is the phase of this resonant interaction. One then finds that an integral of the motion exists, enabling us to write [7]

$$\epsilon\cos\Psi = \Delta - \frac{3}{8}w - \frac{C}{w}, \tag{2.9}$$

where $w = A^2/a^2$, $\Delta = q(p - 2q)a^2/\kappa$, and where the integration constant C is determined by the initial values of w and 2α. By resorting to the envelope equation we can show that $p^2 = 4q^2 + 2\kappa/a^2$ for the breathing mode, so that

$$\Delta = \frac{1}{1 + \sqrt{(1 + k^2/q^2)/2}}, \tag{2.10}$$

where q/k is the tune depression caused by the space charge. In Fig. 1 we plot $\epsilon\cos\Psi$ vs w for $q/k = 0.412$, $\Delta = 0.35$, and various values of C. For $\epsilon = 0.1$, the polar plot of w vs Ψ is shown in Fig. 2. It is clear that Q is an unstable fixed point and that the origin and S are stable fixed points. Figure 2 is equivalent to a "second order stroboscopic plot" for integral values of $pz/2\pi$, and contains the main features of the resonant interaction. Specifically, all trajectories starting within the inner separatrix (thick solid curve) bounded by P and Q oscillate in stable orbits while any trajectory starting just outside will travel along the outer separatrix (thick dashed curve). For these particles, as the amplitude of motion grows the true oscillation wave number increases, enhancing the resonant term and *locking in* to the resonance. And the presence of a thin distribution of trajectories near the outer separatrix has the appearance of a halo in $x - y$ space at the radius corresponding to R in Figs. 1 and 2.

We now drop the simplified model and return to Eq. (2.3). Although the algebra is far more complicated we eventually obtain a more accurate version of Eq. (2.9) with a very similar set of curves to those in Figs. 1 and 2. First we rewrite Eq. (2.3) for the variable $s = r^2/a^2$, obtaining

$$s'' - \frac{(s')^2}{2s} + 2q^2\left(s - \frac{L^2}{s}\right) = -\frac{2\kappa}{a^2}(s-1)\Theta(s-1) + 4\frac{\epsilon\kappa}{a^2}s\cos pz\,\Theta(1-s). \tag{2.11}$$

Guided by the parametrization of the x and y motions separately, the amplitude-phase parametrization of the two-dimensional oscillation is written as

$$s = \frac{w^2 + L^2}{2w} - \frac{w^2 - L^2}{2w}\cos(2qz + \gamma). \tag{2.12}$$

Here w and γ are slowly varying amplitude and phase parameters which would be constant if the right side of Eq. (2.11) vanished. We now write

$$s' = q\frac{w^2 - L^2}{w}\sin(2qz + \gamma) \tag{2.13}$$

and use Eq. (2.11) and the required connection between w' and γ' implied by Eq. (2.13) to obtain explicit expressions for w' and γ'. We then average over oscillations at

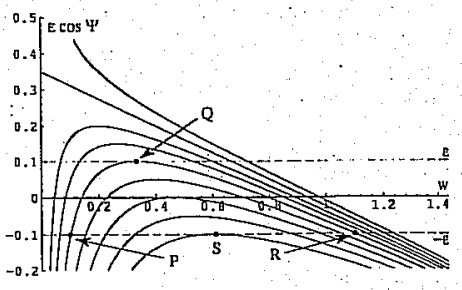

FIG. 1. Plot of $\epsilon\cos\Psi$ vs w for the simplified model with $\Delta = 0.35$.

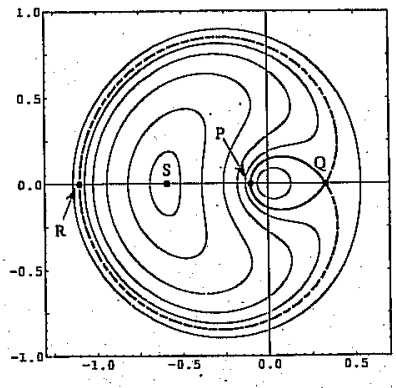

FIG. 2. Polar plot of w vs Ψ for the trajectories corresponding to the parametric resonance using $\Delta = 0.35$, $\epsilon = 0.1$, and the simplified model.

all wave numbers except $2q - p$, being careful to include the step functions as we obtain these averages. The final equations for w' and Ψ' [$\Psi = (2q - p)z + \gamma$] are similar to Eqs. (2.7) and (2.8) and again lead to an integral of the motion, which now is

$$g(1 - h)\epsilon\cos\Psi = f\Delta - t - C, \qquad (2.14)$$

where $f(w) = (w^2 + L^2)/2w$, $g(w) = (w^2 - L^2)/2w$. Here

$$\pi h(w) = \tan^{-1}[\ell/(1 - f)] + \ell(1 - f)/2g^2 \qquad (2.15)$$

for $w \geq 1$ and $\ell(w) = \sqrt{(w - 1)(w - L^2)/w}$. Also

$$t(w) = \frac{1}{\pi}\int_1^w \frac{dw}{wg}\left[(g^2 - f)\tan^{-1}\left(\frac{\ell}{1 - f}\right) + f\ell + L\tan^{-1}\left(\frac{2L\ell}{f - L^2}\right)\right], \qquad (2.16)$$

for $w \geq 1$, and $h(w) = t(w) = 0$ for $w \leq 1$. The arctangents are taken to be in the first or second quadrant. The term in $b(w)$ comes from the amplitude dependence of the ion wave number. A more accurate expression for $b(w)$ can be obtained, if necessary, by solving Eq. (2.6) with $\epsilon = 0$.

Since the resonance will have its greatest effect when $L = 0$, corresponding to ion orbits which pass through the core center, we present a plot of $\epsilon\cos\Psi$ vs w for $\Delta = 0.35$ and $L = 0$ in Fig. 3. The pattern of curves is very similar to that in Fig. 1, and the w, Ψ polar plot in Fig. 4 for $\epsilon = 0.1$ has the same topology as for the simple model in Fig. 2, as is also the case for $L \neq 0$. But the scale for w is about 7 times larger, corresponding to a detuning with amplitude about 7 times smaller than that given by the 3/8 factor in Eq. (2.14).

III. Distribution of L in a symmetric K-V beam.—The distribution in L for a K-V beam is proportional to

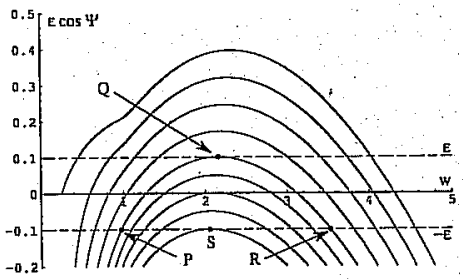

FIG. 3. Plot of $\epsilon\cos\Psi$ vs w for the exact model with $\Delta = 0.35$, $L = 0$.

$$f(L) \sim \int\int\int\int dx\,dy\,dx'\,dy'\,\delta\Big(x^2 + y^2 + \frac{(x')^2}{q^2} + \frac{(y')^2}{q^2} - a^2\Big)\delta(x'y - xy' - Lqa^2). \qquad (3.1)$$

We first do 45° rotations from the x/a, y'/qa space to the u, u' space and from the y/a, x'/qa space to the v, v' space and follow this by integrating over the polar angles in the uv' and vu' spaces. This leads to

$$f(L) \sim \int_0^\infty ds\int_0^\infty dt\,\delta(s + t - 1)\delta\Big(\frac{s - t}{2} - L\Big) = \begin{cases} 1, & 2|L| < 1 \\ 0, & 2|L| > 1 \end{cases}. \qquad (3.2)$$

where $s = u^2 + (v')^2$ and $t = v^2 + (u')^2$ are both positive. Therefore the distribution in L for a K-V beam is uniform from $L = -1/2$ to $L = 1/2$ and vanishes for $|L| > 1/2$.

IV. Implications of the model.—Since the breathing K-V beam is a solution of the Vlasov equation, particles within the core will continue to remain there, even in the presence of the resonant interaction. If however,

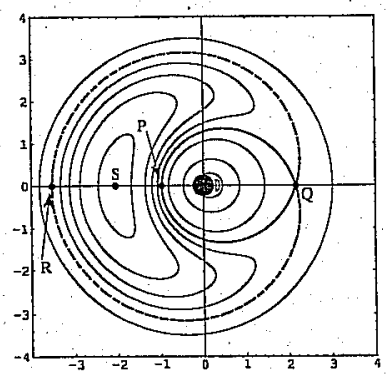

FIG. 4. Polar plot of w vs Ψ for the trajectories corresponding to the parametric resonance using $\Delta = 0.35$, $L = 0$, $\epsilon = 0.1$, and the exact model.

some other mechanism moves the particle outside the core, particularly to an oscillation amplitude exceeding that corresponding to the points P or Q in the figures, a halo will develop at a radius corresponding to point R in the figures. The most likely mechanism to do this is an instability associated with a nonlinear density perturbation. In addition, simulations show that chaotic motion develops near point Q in the figures for a large amplitude breathing mode at high current, enabling particles in the core to populate the halo.

V. Summary and discussion.—We considered a symmetric K-V beam undergoing a breathing mode and found that the parametric resonance ($2q = p$) is a vehicle for particles to leave the core of the beam and perform excursions to large amplitude, forming a distribution in real space in the form of a halo. In this calculation, we neglected the effect of high frequency terms, and the effect of other possible resonances and driving oscillations. Thus our model, which successfully describes a mechanism by which halos can and probably do form, is only an approximation to a much more complicated situation.

We have compared our predictions with some preliminary simulations performed for $L = 0$ by Wangler [8], and find that, for tune depressions from $q/k = 1$ to 0.6, the topology of the stroboscopic plot resembles Figs. 2 and 4 very closely. For tune depressions below 0.6, the stroboscopic plot shows the onset of chaotic behavior in an ever widening band near the inner separatrix as the tune depression deepens. Particles inside but near to the inner separatrix are then able to move outside the inner separatrix and participate more easily in the development of the halo.

Wangler's simulations using a K-V beam [8] confirm that core ions always remain within the inner separatrix. It is quite possible for core ions to lie outside the equivalent inner separatrix for nonuniform equilibrium charge density distributions. We therefore expect the halo mechanisms in the present model to apply to non-K-V beams as well. Lagniel's simulations [6] give similar results, showing the onset of chaos for high space charge as well as the similarity with the three-body astronomical problem.

Our present model is unable to describe either diffusion or chaos in the w, Ψ phase space. If we were to try to do so we would have to include the neglected high frequency terms, as well as resonances other than the one corresponding to the parametric resonance. Integrals of the motion corresponding to Eq. (2.14) would no longer be valid. Descriptions of the growth of halos including the effects of chaos and diffusion will require further analysis and/or extensive numerical simulations.

The author would like to thank Alex Dragt, Bob Jameson, Pierre Lapostolle, Ron Ruth, Rob, Ryne, Fred Skiff, and Tom Wangler for several helpful comments. He is also indebted to Dan Abell for performing the calculations leading to Figs. 1–4.

[1] See I.M. Kapchinsky, *Theory of Resonance Linear Accelerators* (Harford Academic Press, New York, 1985), p. 247ff.

[2] R.A. Jameson, Los Alamos Report No. LA-UR-93-1209 (unpublished). Jameson describes the early observations of emittance growth and halo production, with particular reference to LAMPF simulations and observations.

[3] M. Reiser, in Proceedings of the 1991 Particle Accelerator Conference, San Francisco, California, (unpublished), p. 2497.

[4] A. Cucchetti, M. Reiser, and T. Wangler, in Proceedings of the 1991 Particle Accelerator Conference (Ref. [3]), p. 251.

[5] J.S. O'Connell, T.P. Wangler, R.S. Mills, and K.R. Crandall, in Proceedings of the 1993 Particle Accelerator Conference, Washington, D.C. (unpublished), p. 3657.

[6] J.M. Lagniel, Nucl. Instrum. Methods Phys. Res., Sect. A 345, 46 (1994).

[7] This result can also be obtained using a contact transformation, followed by neglecting rapidly oscillating terms. In fact, the transformed Hamiltonian in the canonical variables w and Ψ is $H = (\kappa/qa^2)[w\epsilon\cos\Psi - \Delta w + 3w^2/8]$.

[8] Tom Wangler (private communication).